UNIVERSITAT POLITÈCNICA DE VALÈNCIA

UNIVERSITAT POLITÈCNICA DE VALÈNCIA

School of Industrial Engineering

Criticality calculation with burnup credit of a PWR spent nuclear fuel pool.

End of Degree Project

Bachelor's Degree in Industrial Engineering

AUTHOR: Cabrera Buenaventura, Ramon

Tutor: Miró Herrero, Rafael

Cotutor: Barrachina Celda, Teresa María

ACADEMIC YEAR: 2023/2024

Abstract

Developments in nuclear technology and engineering have made it possible to increase the energy extracted from uranium in nuclear reactors. Once this energy has reached its maximum, the fuel elements of pressurized water reactors (PWR) are stored in pools filled with borated water, which acts as radioactive shielding and coolant, before being removed permanently from the nuclear power plant site.

In this thesis, the isotopic composition of the spent fuel will be analysed to ensure that it meets nuclear safety and radiological protection standards, following the burnup credit methodology. The burnup inside the reactor will be calculated considering the heterogeneity in the axial power distribution generated in the fuel rods.

POLARIS and KENO-VI codes, belonging to the SCALE 6.2.4 code system, will be used for the calculations and subsequent analysis, respectively.

Keywords: burnup credit, spent fuel, PWR, Criticality, storage pool, safety, POLARIS, KENO-VI, SCALE, Monte Carlo

Resumen

Los avances en ingeniería y tecnología nuclear han permitido aumentar la energía extraída del uranio en los reactores nucleares. Una vez este ha alcanzado su límite, los elementos combustibles de reactores de agua a presión (PWR) son almacenados en piscinas llenas de agua borada, que actúa como blindaje radiactivo y refrigerante, antes de ser retirados definitivamente del recinto de la central nuclear.

En este trabajo se analizará la composición isotópica del combustible gastado para garantizar que cumple las condiciones de seguridad nuclear y protección radiológica empleando la metodología conocida como crédito al quemado. Para ello se calculará el quemado dentro del reactor teniendo en cuenta la heterogeneidad en la distribución axial de potencia generada en las varillas de combustible.

Se utilizarán para los cálculos y posterior análisis, respectivamente, los códigos POLARIS y KENO-VI, pertenecientes al sistema de códigos SCALE 6.2.4.

Palabras clave: crédito al quemado, combustible gastado, PWR, Criticidad, piscina de combustible, seguridad, POLARIS, KENO-VI, SCALE, Monte Carlo

Resum

Els avanços en enginyeria i tecnologia nuclear han permés augmentar l'energia extreta de l'urani en els reactors nuclears. Una vegada este ha aconseguit el seu límit, els elements combustibles de reactors d'aigua a pressió (PWR) són emmagatzemats en piscines plenes d'aigua borada, que actua com a blindatge radioactiu i refrigerant, abans de ser retirats definitivament del recinte de la central nuclear.

En este treball s'analitzarà la composició isotòpica del combustible gastat per a garantir que complix les condicions de seguretat nuclear i protecció radiològica emprant la metodologia coneguda com a crèdit al cremat. Per a això es calcularà el cremat dins del reactor tenint en compte l'heterogeneïtat en la distribució axial de potència generada en les vares de combustible.

S'utilitzaran per als càlculs i posterior anàlisi, respectivament, els codis POLARIS i KENO-VI, pertanyents al sistema de codis SCALE 6.2.4.

Paraules clau: crèdit al cremat, combustible gastat, PWR, Criticitat, piscina de combustible, seguretat, POLARIS, KENO-VI, SCALE, Monte Carlo

Index

List of Figures

List of Tables

Part I

Report

Chapter 1

Introduction

1.1 Precedents.

Energy consumption has been growing exponentially for the last century [1]. This fact led to a massive use of carbon dioxide (CO_2) emitting technologies to supply mankind energy needs.

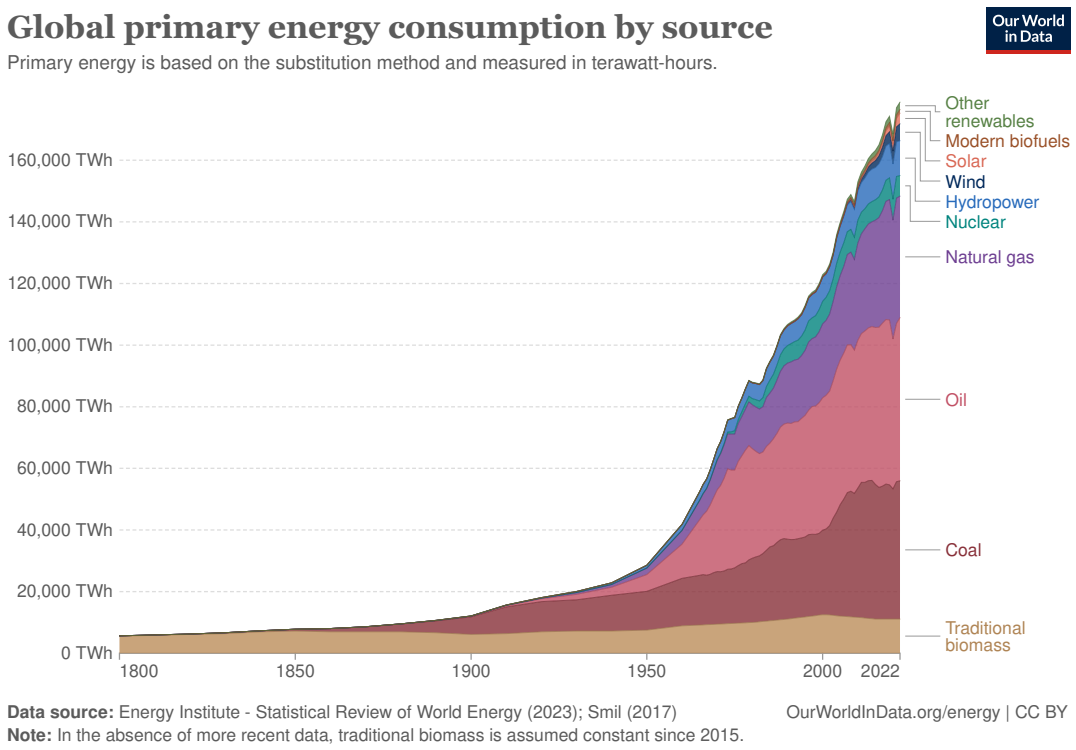

Figure 1.1: Global primary energy consumption by source [1]

While the increasing number of renewable generation installations worldwide is helping to reduce the polluting emissions and contributing to a net-zero energy grid, the role of nuclear energy to reach this goal is also noteworthy. Every year, nuclear power is avoiding the emissions of two gigatonnes of CO_2 around the globe [2].

In Spain, since 1982 all the spent fuel generated in the NPPs has been stored in the corresponding spent fuel pools inside the NPPs site. In view of the forecasts of saturation of the capacity of these pools, throughout the 1990s different projects were carried out for the progressive replacement of the original racks with newer ones more compact and with greater capacity. This allowed, in most cases, the deferral of the need to provide the Spanish system with additional spent fuel storage capacity, thus ensuring the continuity of the operation of the NPPs [3].

Ensuring the safety of these installations is therefore crucial for the management of the NPPs and the protection of the public health and the environment. These pools serve as temporary storage for spent nuclear fuel elements, which remain highly radioactive and thermally hot after their removal from the reactor core. They are filled with water that provides the necessary cooling to dissipate the decay heat of the fuel elements and the radiation shielding to the exterior. During normal operation in PWR NPPs this water also contains boric acid, which act as a neutron absorber and helps lowering the Criticality of the fuel stored.

In this work, the Criticality of an existing spent fuel pool is calculated to ensure compliance with current regulations on nuclear safety and radiation protection when loaded with more enriched fuel from the last operating cycles, following a new approach called the burnup credit methodology. With this method, the burnup of the fuel will be calculated previously, taking into account the difference in power output along its axis, and then the different composition results will be grouped in the spent fuel pool for Criticality calculation.

1.2 Incentive.

The following work has been carried out as a Bachelor's Thesis to obtain the Degree of Engineering in Industrial Technologies of Universitat Politècnica de València (UPV). It has been performed inside the Instituto Universitario de Seguridad Industrial, Radiofísica y Medioambiental (ISIRYM) in close collaboration with the chair of the Consejo de Seguridad Nuclear (CSN), the regulatory authority for nuclear safety and radiation protection in Spain.

Moreover, it has been developed remotely while pursuing an exchange semester at the Eidgenössische Technische Hochschule Zürich (ETH), where more background in the nuclear field has been obtained after taking the course: Technology and Safety of Nuclear Power Plants.

1.3 Justification.

In order to be able to continue using nuclear power in a safely way as an energy source, it is important to keep studying its operating principles and working on nuclear engineering developments.These technological developments have allowed nuclear power plants (NPPs) operators to extract more energy from nuclear fuels, yet the relevant aspects of nuclear safety and radiation protection must be addressed.

In this work, the criticality of the spent fuel generated in a NPP has been calculated and analyzed, taking into account conservative safety measures under the existing nuclear regulatory framework. In the past, these analyses were performed without following the burnup credit methodology, resulting in overly conservative results that did not accurately reflect the true state of the spent fuel in the pool.

1.4 Work structure.

After this introductory section ends, the report takes place. It will start with a theoretical framework, where the essential concepts necessary to understand and develop the project will be explained concisely. Alongside this, a practical framework will describe the tools and codes used during the development of the work.

Next, the specific case study will be introduced and explained, laying the groundwork for the calculations to be conducted in subsequent sections. Following this, the methodology used to obtain the results will be detailed. The report will then present the results, conclusions and future perspectives.

The document will end with the budget and two appendices: the first will contain a relevant unit conversion display, and the second will include the MATLAB© script developed for this work.

1.4.1 Problem statement and opportunity.

Spent fuel of nuclear reactors still contains a considerable amount of fissile material when unloaded from the reactor core. These fissile isotopes, composed mainly by ^{235}U, could potentially form a critical mass after a boron dilution accident if their concentration is high enough [4] or if the spent fuel elements are not stored adequately.

Dealing with this assumption is important in relation to the safety of the nuclear power plant, especially in the use of the spent fuel storage pool during refuelling at the end of each loading cycle.

1.4.2 Constraints.

Several factors influence the criticality of the nuclear fuel in the spent fuel, such as the pool geometry, fuel burnup cycles, initial enrichment,... Most of these parameters are already fixed by the NPP because it is already built, and making a significant design change afterwards would not make economic sense. Therefore, the major tuning parameter that can be modified during the operation of the plant and subsequent spent fuel storage is the burnup. Burnup can be calculated and optimized to comply with all the safety requirements while maximizing the energy extracted from the fuel, thus maximizing economic profitability of the NPP.

1.4.3 Setting of goals.

The main goal of this work is to calculate and ensure that the spent fuel pool of a NPP complies with the safety and regulatory framework. Burnup of the fuel will be calculated following the burnup credit methodology [5]. The calculation sequence developed in this work can also be used in the future to make a further optimization of the burnup strategy and unloading pattern of a nuclear reactor.

Chapter 2

Sustainable Development Goals

2.1 SDGs introduction.

The United Nations Sustainable Development Goals (SDGs) are a set of 17 interlinked global goals designed to be a blueprint to achieve a better and more sustainable future for all. Adopted by all United Nations Member States in 2015, the SDGs address pressing challenges such as poverty, inequality, climate change, environmental degradation, peace, and justice. They represent a universal call to action to end poverty, protect the planet, and ensure that all people enjoy peace and prosperity by 2030 [6]. The SDGs represent a collective effort by all UN member states to create a more equitable and sustainable future, emphasizing the importance of these global challenges and the necessity of a unified approach to solving them. Linking this project to the SDGs highlights its ethical and social implications. Technical achievements are not the only objective, but also contributing positively to society and the environment.

2.2 Relationship with SDGs.

Description of the alignment of the project with the SDGs with a higher degree of relationship:

The integration of criticality calculations with burnup credit of a Pressurized Water Reactor (PWR) spent fuel pool aligns significantly with the SDG 7 and SDG 13.

By maximizing the energy extracted from the fuel elements before being stored, the efficiency of the nuclear fuel cycle can be improved, as well as the operational costs reduced. This is highly related with the SDG 7 - Affordable and clean energy.

When the nuclear energy efficiency is improved, more energy is generated and helps mitigate the emission of greenhouse gases otherwise emitted by fossil fuel sources. Also, accurate criticality calculations ensure that spent fuel is managed safely, minimizing the risk of accidental releases of radioactive material, enhancing the safety and environmental protection, in a close relation with the SDG 13 - Climate action.

Table 2.1: Relationship of the project with Sustainable Development Goals (SDGs).

Sustainable Development Goals	**High**	**Medium**	**Low**	**Not applicable**
1.- No poverty				X
2.- Zero hunger				X
3.- Good health and well-being				X
4.- Quality education				X
5.- Gender equality				X
6.- Clean water and sanitation				X
7.- Affordable and clean energy	X			
8.- Decent work and economic growth			X	
9.- Industry, innovation and infrastructure		X		
10.- Reduced inequalities				X
11.- Sustainable cities and communities		X		
12.- Responsible consumption and production				X
13.- Climate action	X			
14.- Life below water				X
15.- Life on land				X
16.- Peace, justice and strong institutions				X
17.- Partnerships for the goals			X	

Chapter 3

Theoretical background and codes

3.1 Uranium fuel cycle.

The first step in the nuclear power generation industry is mining the uranium ore. After this ore is extracted from the soil, it is crushed and chemically treated in a process called milling. A characteristic yellow cake is obtained, with a concentration of more than 80% of natural uranium.

Nevertheless, this natural uranium contains less than 1% of ^{235}U, the fissile isotope used in nuclear reactors. To increase this percentage to levels between 3-5%, the yellow cake undergoes a series of processes called conversion, where it is transformed into gaseous form uranium hexafluoride (UF_6) and enrichment, where the percentage of ^{235}U increases. The solidified product is then converted into uranium oxide (UO_2) cylindrical pellets, with both diameter and height of about 10 mm. These pellets are packed in tubes about 4 m long to form fuel rods. The fuel rods are grouped into fuel elements, also known as fuel assemblies, and then loaded into the nuclear reactor.

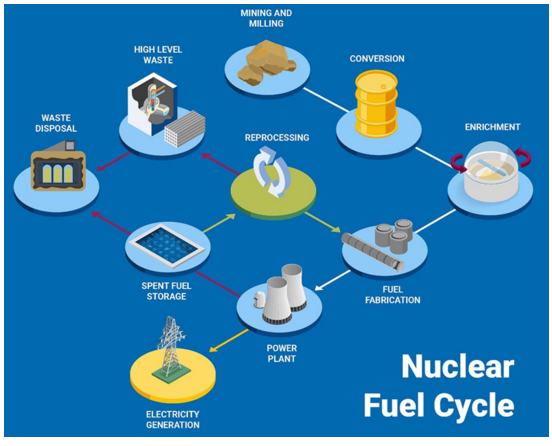

Figure 3.1: IAEA nuclear fuel cycle [7].

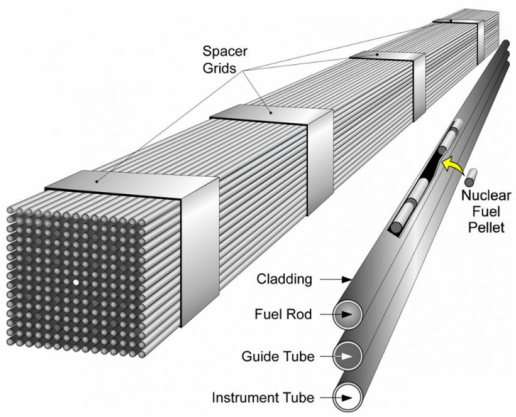

Figure 3.2: 15x15 PWR fuel element overview [8].

After a period of 3 to 6 years of burning, when the fuel cannot be used any longer, it is extracted from the reactor and stored in pools, where water acts both as coolant and radiation shield. Between one-third and one-sixth of the reactor fuel assemblies are replaced at the end of each operating cycle, which lasts approximately one year, in order to completely burn all fuel assemblies at the end of the period.

From these pools, the spent fuel can either be reprocessed and recycled to create new nuclear fuel or be transferred to an interim storage facility. The nuclear waste will be kept in these dry facilities before being disposed deep underground or being burned again in future new generation nuclear reactors.

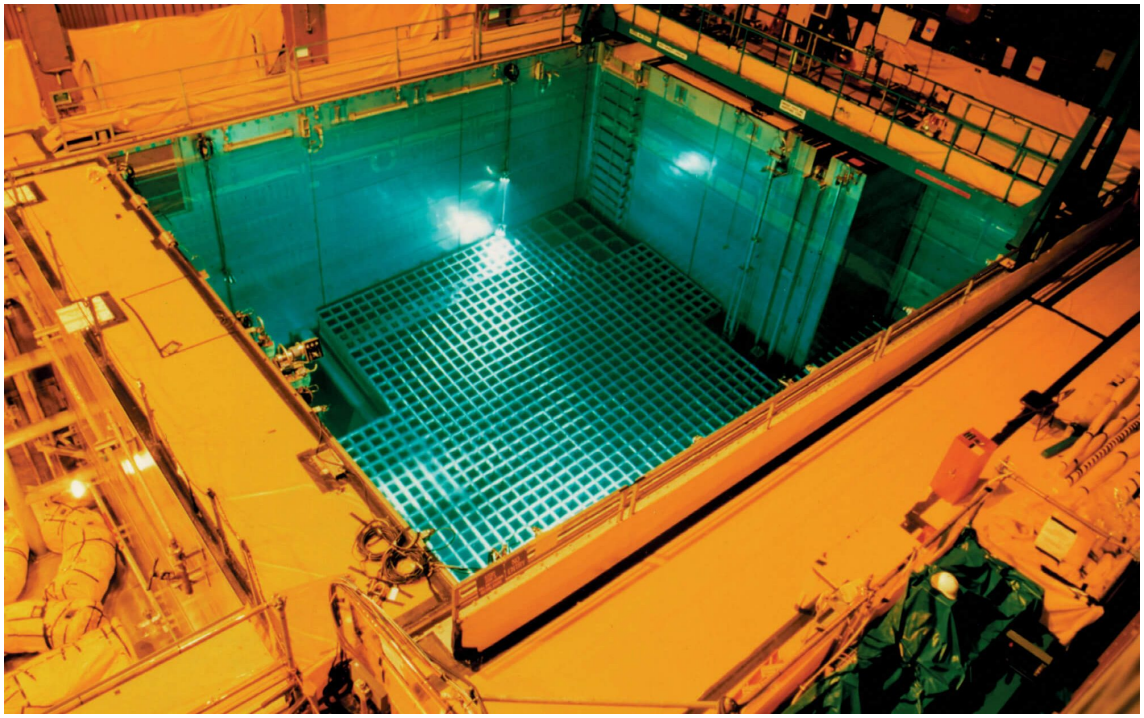

Figure 3.3: Spent fuel pool [8].

Figure 3.4: Dry cask intermediate storage at Connecticut Yankee [8].

3.2 Nuclear power plant operating principles.

In order to understand the physical principles that govern the operation of NPPs, a brief introductory overview is presented in this chapter.

3.2.1 Basics of atoms.

The atom is the fundamental unit of chemical elements. It is composed by positively charged protons, neutrons without electrical charge and negatively charged electrons [9]. The number of protons an atom contains is referred to as the atomic number Z, and it identifies the chemical element. For instance, every atom with 79 protons in its nucleus ($Z = 79$) is an atom of gold.

The mass of a proton and a neutron are approximately equal, while the electron one is negligible. Consequently, we can consider that the mass of the atom is approximately equal to the sum of the masses of the protons and neutrons in its nucleus. It is therefore important to know the total number of protons (N_p) and neutrons (N_n) in the nucleus of an atom. The sum of these numbers is called the mass number and is symbolised by the letter A [10].

$$A = N_p + N_n = Z + N_n \tag{3.1}$$

The standard notation of an atomic nuclei X is denoted by its mass number on the top left and its atomic number on the bottom left, as follows:

$$^{A}_{Z}\mathrm{X}$$

As an example, the atom of uranium ($Z = 92$) with 143 neutrons will be written as: $^{235}_{92}\mathrm{U}$.

In nuclear engineering, the isotopes take a fundamental role. Those are particles of the same element with different weight, due to their varied number of neutrons.

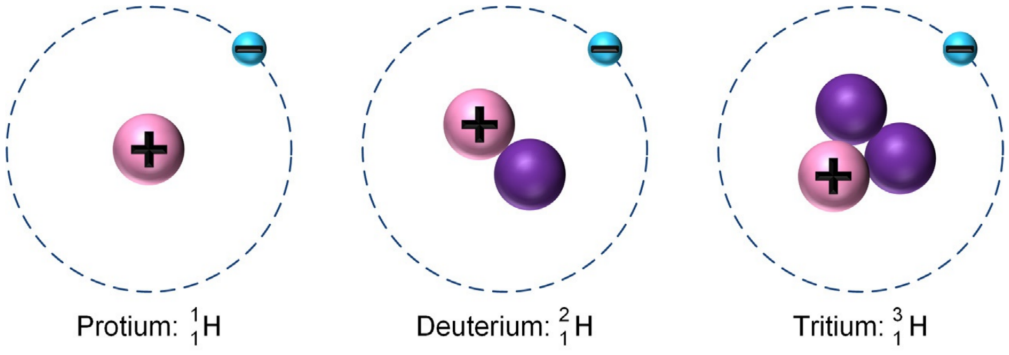

Figure 3.5: Isotopes of Hydrogen [11].

As the number of protons remains the same between isotopes, the atoms will be simply written as the mass number and the chemical element ^{A}X: $^{1}\mathrm{H}, ^{2}\mathrm{H}, ^{3}\mathrm{H}, ^{235}\mathrm{U}, ^{238}\mathrm{U}, \ldots$

Another important notations in the nuclear field are the neutron: $^{1}_{0}\mathrm{n}$ and the electron: $^{0}_{-1}\mathrm{e}$.

It is also convenient to define the energy unit used while dealing with atoms and molecules: the electron-volt (eV). This is the amount of kinetic energy transmitted to an electron (1.60×10^{-19} C) if it is accelerated through a potential difference of 1 volt (V). When dealing with nuclear forces, as they are significantly larger than atomic forces, the mega-electron-volt (MeV) will be used.

$$1\,\text{eV} = qV = (1.60 \times 10^{-19}\,\text{C})(1\,\frac{\text{J}}{\text{C}}) = 1.60 \times 10^{-19}\,\text{J} \tag{3.2}$$

$$1\,\text{MeV} = 1.60 \times 10^{-13}\,\text{J} \tag{3.3}$$

3.2.2 Basics of radioactivity and transmutation.

Many isotopes are unstable, specially the ones of heavy elements, and have the property of radioactivity. This is the spontaneous decay of the atom with the emission of a particle. There exists three types of radioactive decay: α (alpha), β (beta) and γ (gamma) [11].

In an α-decay process, a helium nucleus is emitted as the particle, labeled as the α particle:

$$^{238}_{92}\text{U} \longrightarrow {}^{234}_{90}\text{Th} + {}^{4}_{2}\text{He} \tag{3.4}$$

The β-decay is merely the emission of an electron, called the β particle when it arises in a nuclear process. This process is originated by the conversion of a neutron into a proton and an electron, plus a neutrino in this particular example:

$$^{234}_{90}\text{Th} \longrightarrow {}^{234}_{91}\text{Pa} + {}^{0}_{-1}\text{e} + \nu \tag{3.5}$$

In a γ-decay, an excited nucleus get rid of excess internal energy by the emission of a gamma ray (photon), and the atomic and mass number remain the same.

On top of the above, there are also the X-rays, a kind of γ radiation produced by artificial means, and the neutron radiation, where neutrons are ejected from the atom after some triggering event, like a nuclear fission. [12]

The number of disintegrations per second that occurs in a radioisotope sample is called the activity, A, and is measured in becquerel (1 Bq = 1 disintegration per second). As this sample decreases at a rate proportional to its current number of atoms, its decay is exponential. The rate of this decay is called the radioactive decay constant, λ (s^{-1}), and it is related to the half-life, $t_{1/2}$, the time it takes to reduce to half the initial number of atoms:

$$t_{1/2} = \frac{\ln(2)}{\lambda} \tag{3.6}$$

For N nuclei, the activity is the result of multiplying the quantity of atoms times the chance of decay, the decay constant λ:

$$A = \lambda N \tag{3.7}$$

All of these events are referred to as ionizing radiation, as they carry enough energy than they can knock out electrons from the orbits of the atoms and form electrically charged particles called ions. When ionizing radiation interacts with cells, it can damage them and damage genetic material [13], thus protection of the radioactive sources is crucial for the safety and health of the public and NPP workers.

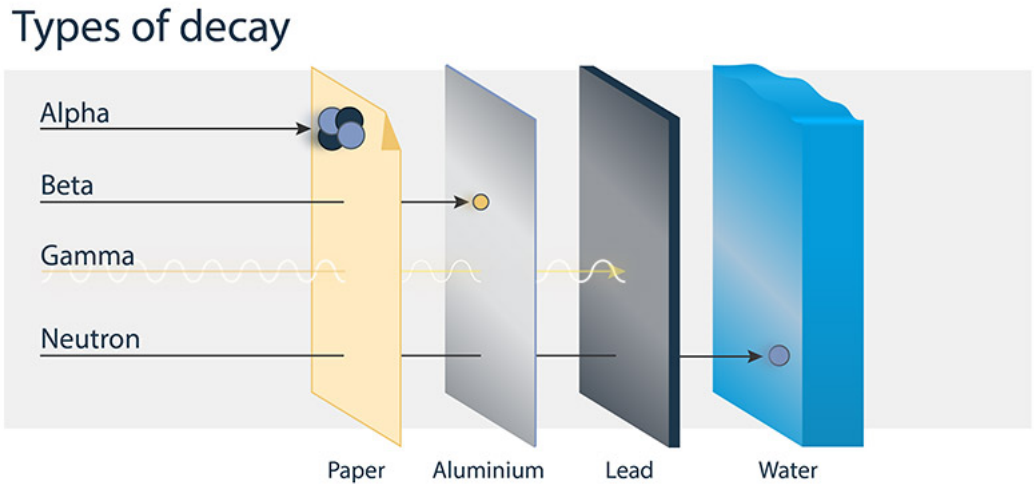

Figure 3.6: Types of ionizing radiation and their means of protection [12].

If all these nuclear reactions take place spontaneously are referred as radioactivity. Nevertheless, the same kind of reactions can be induced by bombardment of the atoms with a particle or ray. The result is the conversion of one element into another, in a process called transmutation.

This process was first achieved by Rutherford in 1919 [14], when he bombarded nitrogen atoms with an α radioactive source, obtaining oxygen and a proton:

$$ {}^{4}_{2}\mathrm{He} + {}^{14}_{7}\mathrm{N} \longrightarrow {}^{17}_{8}\mathrm{O} + {}^{1}_{1}\mathrm{H} \tag{3.8} $$

It should be noted that it is difficult for the positively charged α particle to enter the nitrogen nucleus because of the electrical repulsion between charged particles. Neutrons, being neutral particles and not experiencing any electrostatic repulsion, are especially useful as projectiles to penetrate a target nucleus and induce nuclear reactions.

The chance of collision of a neutron with a target atom is called the microscopic cross section σ, and it is measured in barn (1 barn $= 10^{-28}$ m^2). Whenever a collision occurs, the neutron can either scatter the atom (σ_s), being absorbed by it (σ_a) or trigger a fission reaction (σ_f). Each of these events being chances of reaction, their sum is the total cross section of the atom.

$$ \sigma = \sigma_a + \sigma_s + \sigma_f \tag{3.9} $$

3.2.3 The fission chain reaction and moderation.

The absorption of a neutron involves the start of an excited state in the atom, with the extra energy being released as gamma rays. In some heavy elements, notably uranium and plutonium, the excited state can trigger the splitting of the nucleus into two lighter nuclei in a process called fission.

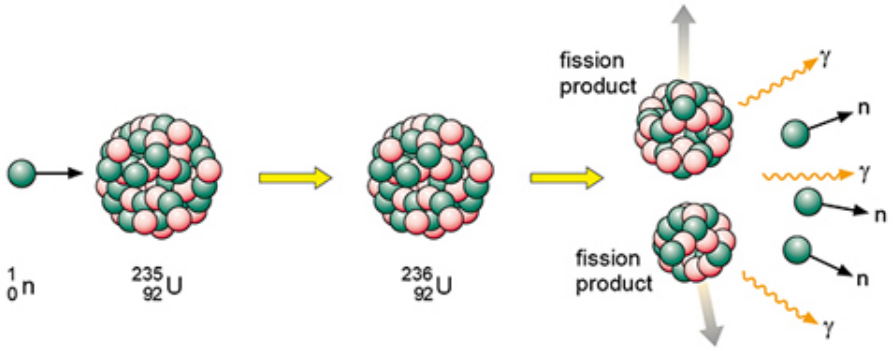

Figure 3.7: Fission of a ^{235}U atom [15].

The byproducts of fission, mainly radioactive isotopes, are called fission products. The distribution of the composition of these products is known as the fission yield.

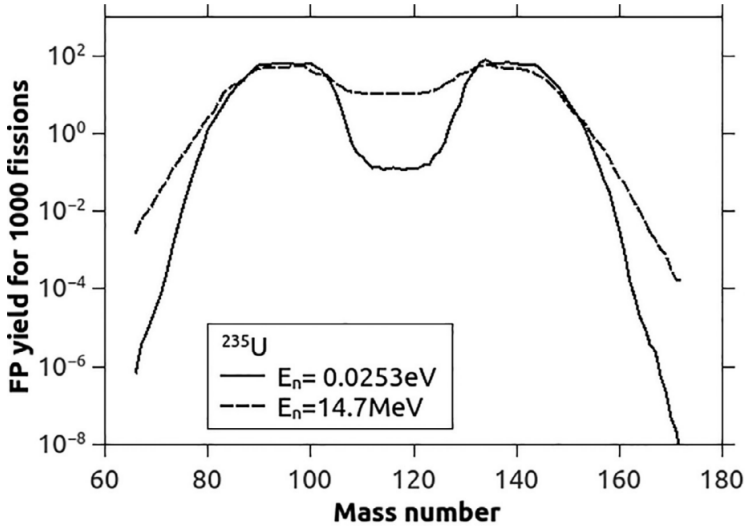

Figure 3.8: Fission product yields for 1000 fissions in ^{235}U at two neutron energies.[16].

In the ^{235}U fission showed in Figure 3.7, approximately 200 MeV of energy are released on average, providing the main source of energy in nuclear reactors. Even though about 10 MeV of this energy escape the reactor in form of neutrinos, around 190 MeV are still effectively available [11].

It is remarkable that by the conservation of mass-energy ($E = mc^2$), the mass of the sum of the byproducts is smaller than the nucleus from which they emerge, and the defect in mass constitutes the energy released. A common release of fission products when ^{235}U undergoes nuclear fission is the following (Eq. 3.10):

$$^{235}_{92}\mathrm{U} + ^{1}_{0}\mathrm{n} \longrightarrow ^{90}_{36}\mathrm{Kr} + ^{144}_{56}\mathrm{Ba} + 2\,^{1}_{0}\mathrm{n} + \mathrm{E} \tag{3.10}$$

Table 3.1: Masses distribution of ^{235}U fission in Eq. 3.10.

Element	$^{235}_{92}$**U**	$^{1}_{0}$**n**	$^{90}_{36}$**Kr**	$^{144}_{56}$**Ba**	**2** $^{1}_{0}$**n**	**E**
Mass (amu) [17]	235.04392	1.00867	89.91952	143.92295	2.01734	0.19278

In this particular example, the mass defect is equal to 0.19278 atomic mass units (amu). As 1 amu = 931.5 MeV [Annex 1], the energy released in this nuclear fission is equal to 179.57457 MeV.

Besides the fission products, 2.42 neutrons are released on average in the fission of ^{235}U with thermal neutrons. This is due to the so-called neutron excess phenomena. Neutrons compensate the electrostatic forces between positively charged protons. Stable light elements have equal numbers of protons and neutrons, but when the number of protons increases, the electrostatic forces also grow and a higher number of protons is needed to stabilize the nucleus. When a fission occurs, a heavy element is transformed into two lighter ones that need a smaller neutrons/protons ratio to be stable. This neutron excess is the origin of the β-decay of the fission products.

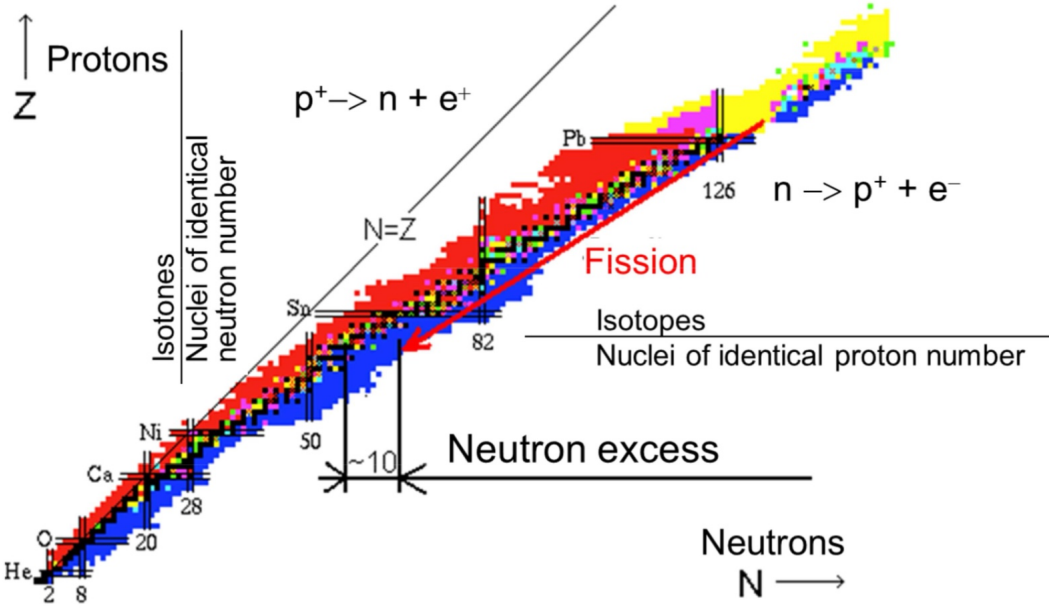

Figure 3.9: Nuclide chart (Courtesy of A. Manera of ETH Zürich) [18].

These neutrons produced by nuclear fission are fast (they carry a high amount of energy, about 2 MeV), but the cross sections to induce another nuclear fission are dependent on energy as shown below (Figure 3.10):

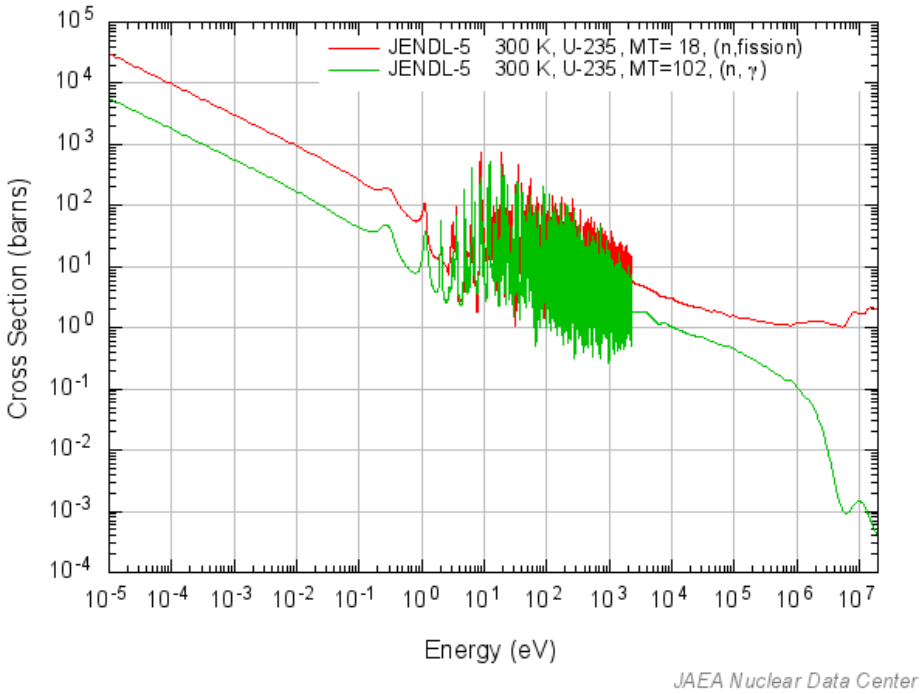

Figure 3.10: Energy dependency of ^{235}U fission and absorption cross sections [19].

Therefore, to use the fast neutrons arisen in the first fission reaction to induce subsequent fission reactions, forming the event known as chain reaction, neutrons must be slowed down to very low energies, obtaining a very high chance of fission (cross section σ_f, red line in Figure 3.10). Slow neutrons are also called thermal neutrons, and when an isotope can be fissioned with them is called fissile, such as ^{235}U.

In thermal nuclear reactors, a reactor moderator is utilized to slow down fast reactors. It is formed by a light element that, by colliding with the neutrons, slows them until they carry an energy favorable for fission. A wide variety of light elements can be used as moderator. In pressurized water reactors (PWR), such as the one studied in this work, the moderator utilized is light water.

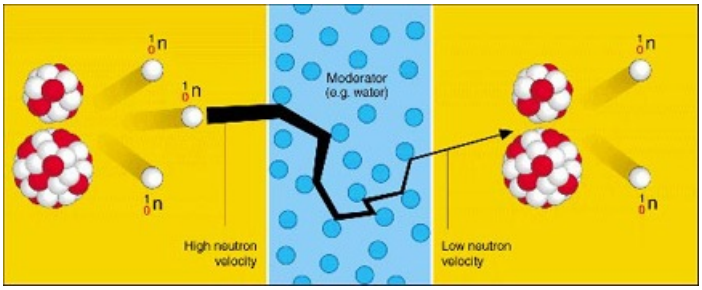

Figure 3.11: Representation of the fission chain reaction due to the slowing down of neutrons in the moderator [20].

3.2.4 Criticality and reactivity.

To analyze the fission chain reaction state, a single number k_{eff} (or k) known as the effective neutron multiplication factor tells the net number of neutrons per initial neutron. This value is function of several factors such as reactor geometry, operating temperature, isotopes cross sections, leakage factors, moderator,... that influence the overall system.

In a nuclear reactor the goal is to provide a steady state power output, thus the desired k_{eff} value is 1, maintaining constant the number of fission reactions. In this state the system is referred to as critical.

$$\begin{aligned} k_{eff} &< 1 \text{ subcritical} \\ k_{eff} &= 1 \text{ critical} \\ k_{eff} &> 1 \text{ supercritical} \end{aligned}$$

Regarding the safe storage of spent nuclear fuel and fissionable material, the value of k_{eff} must be kept well below 1, in a subcritical state, in order to not incur in an uncontrolled grow of fission reactions and a consequently power excursion.

To describe the changes in the criticality a term called reactivity ρ is defined as the deviation of the effective multiplication factor from unity:

$$\rho = \frac{k_{eff} - 1}{k_{eff}} = \frac{\Delta k_{eff}}{k_{eff}} \tag{3.11}$$

To operate a nuclear reactor, large amounts of fuel must be present for the chain reaction to take place and achieve criticality. Given that no fuel is added during the operating cycle, all the fuel of the operating cycle must be installed at the beginning. The first amount of fuel is added to the reactor, and the rest of the fuel causes a supercritical state. In PWR reactors, this excess of reactivity is reduced by using the control rods or, more conveniently, injecting a solution of boron (neutron absorber) into the water to maintain the overall k_{eff} of the system equal to 1.

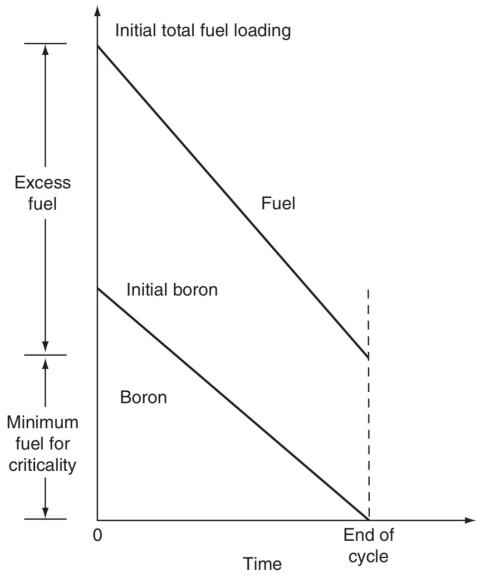

Figure 3.12: Reactivity control during operation in PWR [11].

3.2.5 PWR heat transfer and electricity generation.

The total energy each fuel assembly provides by nuclear fissions is defined as the burnup, and measured in mega-watts day (MWd). The energy released per unit mass is called specific burnup and measured in mega-watts day per metric ton of initial heavy metal ($\frac{\text{MWd}}{\text{MTHM}}$).

Now that the principles of nuclear energy generation have been introduced, it is important to understand how this energy is transferred to the water around the reactor core to later produce steam and generate electricity.

In a typical NPP delivering 1000 MW_e to the grid, around 3000 MW_th are produced. This heat generated in the fission is transported inside the nuclear fuel by conduction (Eq. 3.12):

$$Q = \frac{k}{x} \cdot A \cdot \Delta T \tag{3.12}$$

Where:

Q = heat flow (W)
k = thermal conductivity ($\frac{\text{W}}{\text{mK}}$)
x = thickness (m)
A = cross-sectional area (m^2)
ΔT = temperature difference between fuel pellet and fuel rod

It is important to notice that these are first order simple approximations to explain the overall working principles of NPPs, real processes are way more complex and are affected by several factors. For instance, there is a small gap between the fuel pellets and the fuel rod filled by helium gas, with a very poor thermal conductivity, and that will enlarge the temperature drop. Also, the thermal conductivity is not constant and varies with temperature, therefore it varies with the axial position in the fuel pin. Both these assumptions are addressed in the posterior work analysis.

The heat flux that reaches the clad surface is then transferred to the coolant (water, that acts both as a coolant and a moderator) by convective heat transfer (Eq. 3.13):

$$Q = h \cdot A \cdot (T_s - T_c) \tag{3.13}$$

Where:

Q = heat flow (W)
h = convective heat transfer coefficient ($\frac{\text{W}}{\text{m}^2\text{K}}$), dependent on the water flow regime
A = heat transfer area (m^2)
T_s = temperature of the fuel rod surface
T_c = temperature of the coolant

As the water flows along the reactor core, it absorbs thermal energy and its temperature rises. Due to the principle of conservation of energy we can obtain the temperature values of the water outlet. This temperature and mass flow will be used later to generate steam in the steam generator (Eq. 3.14):

$$Q = \dot{m} \cdot c_p \cdot (T_{out} - T_{in}) = \dot{m} \cdot (h_{out} - h_{in}) \tag{3.14}$$

Where:

Q = heat flow (W)
$\dot{m}$ = mass flow of the coolant ($\frac{\text{kg}}{\text{s}}$)
c_p = specific heat capacity ($\frac{\text{J}}{\text{kg K}}$)
T_{out} = temperature of the hot leg, water outlet
T_{in} = temperature of the cold leg, water inlet
h_{out} = specific enthalpy of the hot leg, water outlet ($\frac{\text{J}}{\text{kg}}$)
h_{in} = specific enthalpy of the hot leg, water outlet ($\frac{\text{J}}{\text{kg}}$)

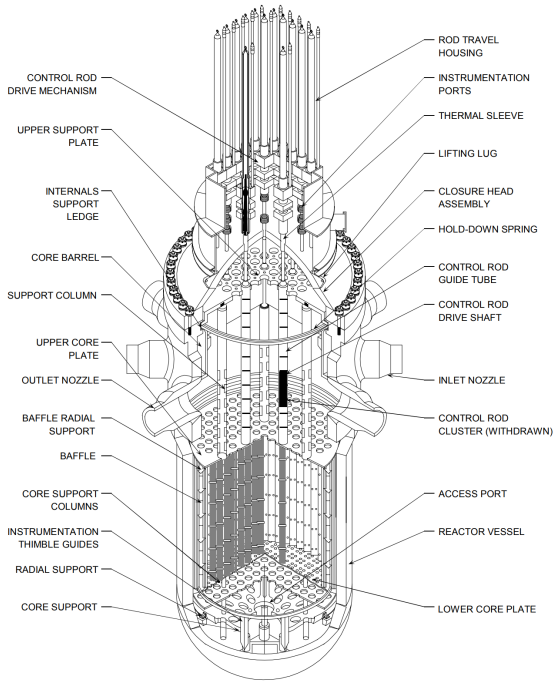

Figure 3.13: Cutaway View of PWR Reactor Vessel [21].

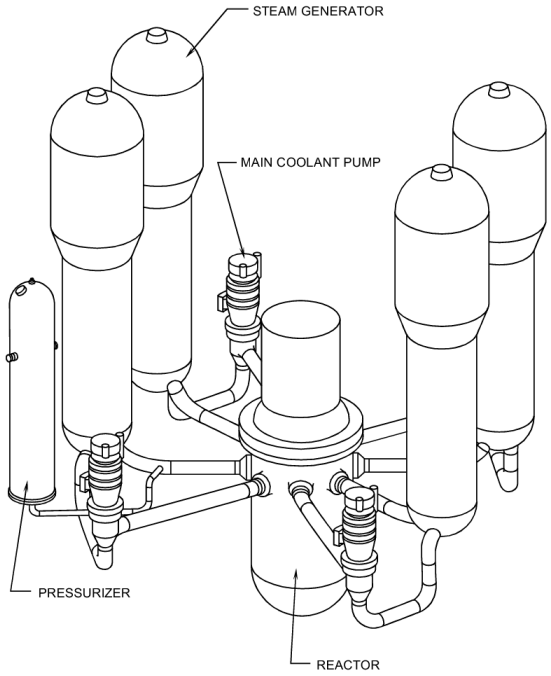

Figure 3.14: Scheme of a 4-loop Westinghouse PWR [21].

In PWR reactors, in order to not reach the saturation point and form bubbles that reduce the heat transfer coefficient, water is running at a high pressure (about 15 MPa) in the primary circuit. This pressure is regulated and kept constant thanks to the pressurizer. The heated water coming out of the reactor goes into a steam generator, where water in the secondary circuit gets converted into steam. This steam turns a series of turbines coupled to a generator that delivers the electricity output. There is also a tertiary circuit that allows for the condensation of the steam turbine outlet to keep generating steam again.

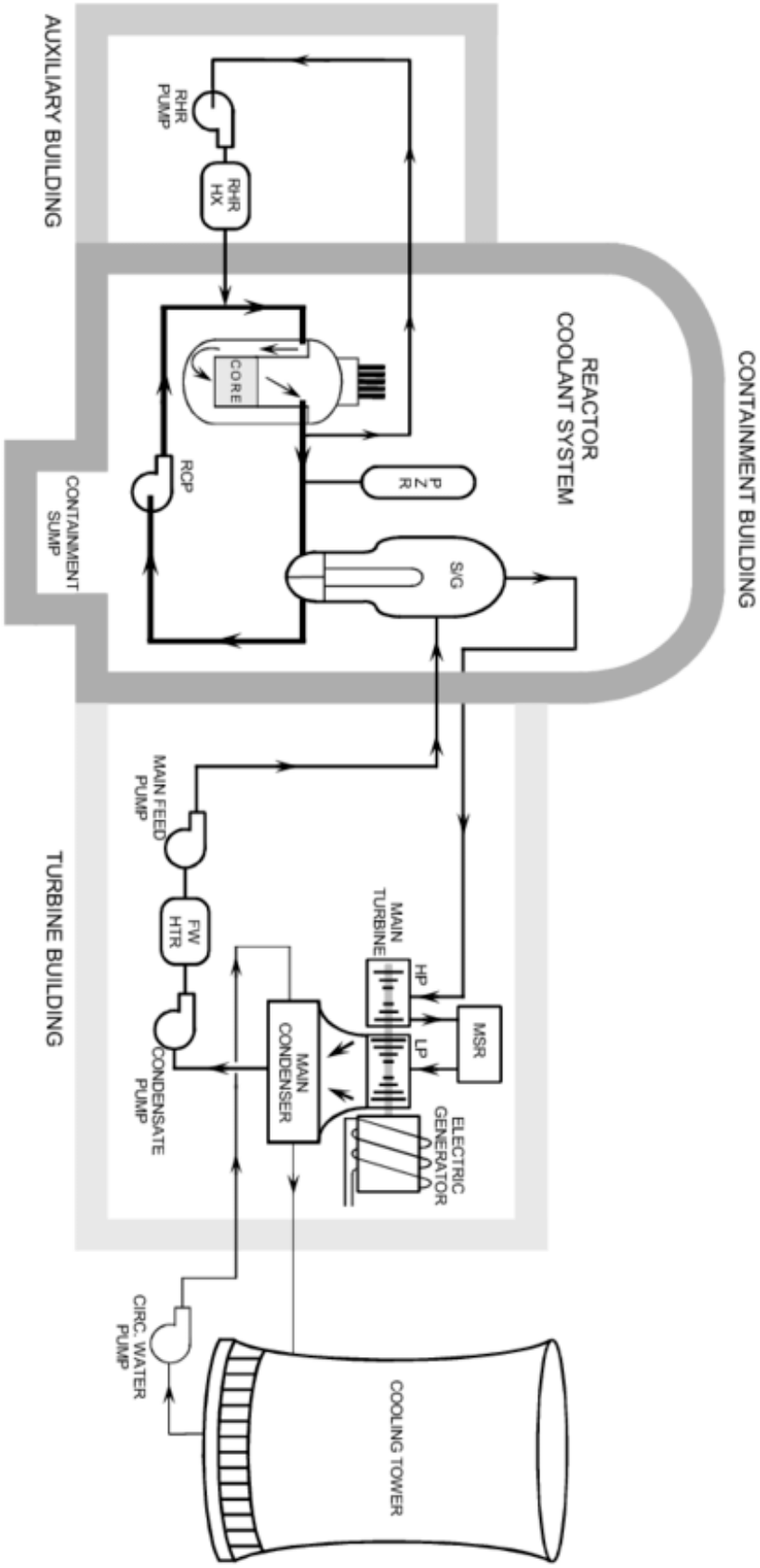

Figure 3.15: Scheme of a PWR NPP [21].

3.3 Neutron transport theory.

The time-dependent process by which nuclides transmute under irradiation is known as depletion or burnup. While analyzing the burnup of the nuclear fuel inside a reactor there are multiple factors that take place at the reaction level. This neutron flux phenomena can be predicted with the Boltzmann transport equation, formulated as additions and substractions in a given increment of space r, energy E, direction Ω and time t:

$$\begin{aligned}\frac{1}{v(E)}\frac{d\phi(r,E,\Omega,t)}{dt}\ ① &= -\Omega\nabla\phi(r,E,\Omega,t)\ ② - \Sigma_t(r,E,\Omega)\phi(r,E,\Omega,t)\ ③ \\ &+\chi(E)\int_{E'}dE'\int_{\Omega'}d\Omega' v\Sigma_f(r,E',\Omega')\phi(r,E',\Omega',t)\ ④ \\ &+\int_{E'}dE'\int_{\Omega'}\Sigma_s(r;E'\rightarrow E;\Omega'\rightarrow\Omega)\phi(r,E',\Omega',t)\ ⑤\end{aligned} \tag{3.15}$$

Where:

Term 1 = rate of accumulation of neutrons
Term 2 = rate of leakage out of the volume
Term 3 = removal due to absorption or scatters
Term 4 = total fission rate, χ(E) refers to the energy spectrum produced in the fission process
Term 5 = differential scattering of neutrons from initial energy E' to final energy E, and from initial direction Ω' to final direction Ω

In essence, it claims that neutrons gained equals neutrons lost inside a given volume. Even though it can be relatively simple to derive, it is computationally high demanding and hard to solve with deterministic methods. In order to be solved by computational methods, the overall ordinary differential equations (ODEs), known as Bateman equations, that describe nuclide generation, depletion and decay can be written as:

$$\frac{dN_i}{dt} = \sum_{j\neq i}(l_{ij}\lambda_j + f_{ij}\sigma_j\Phi)N_j(t) - (\lambda_i + \sigma_i\Phi)N_i(t) + S_i(t) \tag{3.16}$$

Where:

N_i = amount of nuclide i
λ_i = decay constant of nuclide i ($\frac{1}{s}$)
l_{ij} = fractional yield of nuclide i from decay of nuclide j
σ_i = spectrum-averaged removal cross section for nuclide i (barn)
f_{ij} = fractional yield of nuclide i from neutron-induced removal of nuclide j
Φ = angle- and energy-integrated time-dependent neutron flux ($\frac{neutrons}{cm^2\cdot s}$)
S_i = time-dependent source/feed term ($\frac{atoms}{s}$)

And then conveniently rewritten once more in a matrix form as:

$$\frac{d\vec{N}}{dt} = A\vec{N}(t) + \vec{S}(t) = (A_{\sigma,n}\Phi_n + A_\lambda)\vec{N}(t) + \vec{S}(t) \tag{3.17}$$

to be solved by computational methods. A is referred to as the transition matrix. It can be represented as the part containing the reaction terms $A_{\sigma,n}$ and the part containing the decay terms A_{λ}.

3.4 Monte Carlo and deterministic transport solutions.

In order simulate a nuclear reactor two primary methods are used: deterministic and Monte Carlo methods. Their applications depend on the specific goals of the simulation.

Deterministic methods solve equations (such as the neutron depletion equation, Eq. 3.16) directly, within a fixed mathematical framework. In this case, the core of the reactor is split into axial nodes (subdivisions) and the simplified equation is solved within each node. It also ensures continuity between nodes due to the boundary conditions present at the frontiers. This method requires less computational power because of its simplifying assumptions, but can reduce the overall accuracy of the results.

Monte Carlo methods use statistical sampling to solve equations. In the case of the neutron depletion equation, instead of solving the equation directly, they simulate the paths of a large number of neutrons as they move through the reactor. This method, on the other hand, provides a higher accuracy on the results at the expense of a process computationally intensive.

Note that these results, obtained in a statistical way, provide not only a k_{eff} value (Ks) but also a statistical range quantified by the the standard deviation (σ). The maximum k_{eff} value is calculated by adding twice the standard deviation (2σ, ΔKs) to the k_{eff} value. This gives a conservative estimate accounting for the statistical uncertainty:

$$\text{MAX } k_{eff} = k_{eff} + 2\sigma \tag{3.18}$$

In addition, the code validation process yields an average value Kc for various critical experiments where true $k_{eff} = 1$, and a statistically derived uncertainty ΔKc. Defining the mean bias of the code as the difference $(1 - \text{Kc})$ and ΔKc as its uncertainty, the confidence limit of k_{eff} shall be calculated with an equation including both direct uncertainties and those associated with the code itself. In order to comply with the regulations, the mean bias of the code is not taken if its value is negative, because of conservative reasons. True value of k_{eff} shall be below the maximum k_{eff} value calculated + uncertainties with a 95% probability, at the 95% confidence level. This limit value is calculated with Eq. 3.19:

$$k_{eff}\ (95/95) = \text{Ks} + (1 - \text{Kc}) + \sqrt{(\Delta\text{Kc})^2 + (\Delta\text{Ks})^2} \tag{3.19}$$

The values of the uncertainty coefficients for the codes used [22], validated with data from real experiments, are found in next Table 3.2:

Table 3.2: Uncertainty coefficients for the Monte Carlo code used

	Number of experiments	1-Kc	ΔKc
UNBORATED	88	-0.00163	1.23448×10^{-3}
BORATED	25	0.0032328	1.61443×10^{-3}

In this work both solving methods are combined. A deterministic method (POLARIS code) is used to calculate the burnup inside the nuclear reactor following the burnup credit methodology. The results are then translated into a Monte Carlo method (KENO-VI code) that is used to calculate the criticality (k_{eff}) of the spent fuel stored in the spent fuel pool, ensuring that it meets nuclear safety and radiological protection standards.

3.5 Spent fuel safety.

In the case studied in this work, the original pool was divided into two storage regions. The first region intended for the storage of fresh and spent fuel assemblies and the second one for the storage of completely depleted fuel assemblies. Is in this second region where the calculated fuel elements are meant to be stored.

Criticality safety analyses for spent fuel pool storage may utilize one of two available approaches [23]:

1. For pools where no credit for soluble boron is taken (typically BWR pools), the criticality safety analyses must meet the following limit:

   (a) With the spent fuel storage racks loaded with fuel of the maximum fuel assembly reactivity and flooded with unborated water, the k_{eff} must not exceed 0.95, at a 95 percent probability, 95 percent confidence level.

   $$k_{eff}\ (95/95)\ \leq 0.95$$

2. For pools where credit for soluble boron is taken (typically PWR pools), the criticality safety analyses must meet two independent limits:

   (a) With the spent fuel storage racks loaded with fuel of the maximum fuel assembly reactivity and flooded with unborated water, the k_{eff} must remain below 1.0 (subcritical), at a 95-percent probability, 95 percent confidence level.

   $$k_{eff}\ (95/95)\ \leq 1$$

   (b) With the spent fuel storage racks loaded with fuel of the maximum fuel assembly reactivity and flooded with borated water, the k_{eff} must not exceed 0.95, at a 95-percent probability, 95-percent confidence level.

   $$k_{eff}\ (95/95)\ \leq 0.95 \text{ (0.98 in accident conditions [24])}$$

3.6 Regulations.

The following regulations are applicable to criticality analyses for nuclear fuel storage at LWR facilities and are provided in the Title 10 of the Code of Federal Regulations (10 CFR) of the U.S. Nuclear Regulatory Commission (NRC) [25]:

- (10 CFR) 50 Appendix A, General Design Criteria for Nuclear Power Plants Criterion 1, “Quality Standards and Records.”
- (10 CFR) 50 Appendix A, General Design Criteria for Nuclear Power Plants Criterion 2, “Design Bases for Protection Against Natural Phenomena.”
- (10 CFR) 50 Appendix A, General Design Criteria for Nuclear Power Plants Criterion 3, “Fire Protection.”
- (10 CFR) 50 Appendix A, General Design Criteria for Nuclear Power Plants Criterion 4, “Environmental and Dynamic Effects Design Bases.”

- (10 CFR) 50 Appendix A, General Design Criteria for Nuclear Power Plants Criterion 5, “Sharing of Structures, Systems and Components.”
- (10 CFR) 50 Appendix A, General Design Criteria for Nuclear Power Plants Criterion 61, “Fuel Storage and Handling and Radioactivity Control.”
- (10 CFR) 50 Appendix A, General Design Criteria for Nuclear Power Plants Criterion 62, “Prevention of Criticality in Fuel Storage and Handling.”
- (10 CFR) 50 Appendix B, “Quality Assurance Criteria for Nuclear Power Plants and Fuel Reprocessing Plants.”
- (10 CFR) 50.68, “Criticality Accident Requirements.”
- (10 CFR) 50.36, “Technical Specifications.”
- (10 CFR) 52.47(a)(17), “Contents of applications; technical information.”; 52.79(a)(43), “Contents of applications; technical information in final safety analysis report.”; 52.137(a)(17), “Contents of applications; technical information.”; and 52.157(f)(8), “Contents of applications; technical information in final safety analysis report.”
- (10 CFR) 70.24, ”Criticality Accident Requirements.” (for license applications)

In relation with the spanish regulations, UNE 73501:1992 ”Criticality requirements for the design of fuel racks.” and its 2009 Erratum are applicable. In addition, for the project development, it is advisable to follow UNE 157001:2014 : ”General criteria for the formal preparation of the documents constituting a documents constituting a technical project”.

For the development of this work, the main safety requisites are found in (10 CFR) 50.68 ”Criticality Accident Requirements” segment.

3.7 Codes.

3.7.1 SCALE 6.2.4.

In order to perform the computational calculation and analysis of the PWR spent fuel pool the code system SCALE (version 6.2.4) is used. SCALE is a comprehensive modeling and simulation suite for nuclear safety analysis and design developed and maintained by Oak Ridge National Laboratory (ORNL) to perform reactor physics, criticality safety, radiation shielding, and spent fuel characterization for nuclear facilities and transportation/storage package designs [26].

This code system has been accessed and run remotely through the ISIRYM Quasar via the UPV VPN, where a Linux environment contains a distribution of SCALE installed, including all the data libraries required.

3.7.2 ORIGEN.

ORIGEN (Oak Ridge Isotope Generation code) is a SCALE module that calculates time-dependent concentrations, activities, and radiation source terms for a large number of isotopes simultaneously generated or depleted by neutron transmutation, fission, and radioactive decay. It is widely used in both industry and research.

ORIGEN calculates, in a deterministic way, time-dependent concentrations, activities, and radiation source terms for a large number of isotopes simultaneously generated or depleted by neutron transmutation, fission, and radioactive decay.

3.7.3 OBIWAN.

OBIWAN (Origen Binary Interrogation Without A scale iNput) is a command-line utility for viewing, manipulating, and converting ORIGEN binary output files. It will be used to convert the ".f71" ORIGEN binary output file into a ".csv" file in order to perform analysis of the output data.

3.7.4 POLARIS.

Polaris is a capability for SCALE that provides two-dimensional (2D) lattice physics analysis for light water reactor (LWR) fuel designs. It uses the Embedded Self Shielding Method (ESSM) for multigroup cross section processing and a transport solver based on the Method of Characteristics (MOC). Polaris is integrated with ORIGEN for depletion calculations.

Using Polaris the isotopic composition of the fuel rods after an operating cycle can be obtained. This is referred to as the burnup calculation. The composition is then translated into KENO-VI code to perform the corresponding criticality analysis.

3.7.5 CSAS6.

The Control Module For Enhanced Criticality Safety Analysis Sequences (CSAS) with KENO code provide reliable and efficient means of performing k_{eff} calculations for systems that are routinely encountered in engineering practice. This sequence implements the module XSProc (the material and cross section processing module of SCALE) to process material input and provide a temperature and resonance-corrected cross-section library based on the physical characteristics of the problem being analyzed. The geometric modeling capabilities available in KENO codes coupled with the automated cross-section processing within CSAS allow complex, 3D systems to be analyzed.

3.7.6 KENO-VI.

KENO (version VI) is a three-dimensional (3D) Monte Carlo Criticality transport program developed and maintained for use as part of the SCALE Code System. It is used to calculate k_{eff}, fluxes, reaction rates and other data for 3D systems. KENO-VI is run as a part of a CSAS sequence. KENO codes are executed to calculate the k_{eff} factor using the cross-section library that was prepared by the CSAS sequence.

Chapter 4

PWR spent fuel storage pool analysis

Two PWR fuel elements, type A and type B (each one presenting different values of burnup), with an initial enrichment of 5% ^{235}U and the exact same geometry will be calculated with the POLARIS code during 5 operating cycles of 1 year.

The fuel elements will be segmented into 32 equal parts in size, with different values of power delivered to represent more accurately the power distribution along the axis of the fuel rods (Figure 4.1).

The composition output at the end of the 5 years period will then be translated to KENO-VI to calculate the k_{eff} values inside the pool where the spent fuel assemblies are meant to be stored.

4.1 Fuel element composition and power distribution.

When the fuel elements are introduced into a PWR reactor, the neutron flux typically forms a sine wave shape, resulting in a higher burnup level at the center of the assembly compared to its ends. This flux shape is influenced by several factors, including neutron leakage at the ends and the concentration of fission products in the central region of the fuel element. Due to this, the ends of the spent fuel remain the most reactive regions due to their lower burnup and neutron loss during irradiation. This effect results in a characteristic axial burnup distribution, featuring a plateau in the central part of the fuel element and two slopes with lower burnup levels at the ends. To numerically approximate the axial isotopic variation, the profile must be discretized into segments, with each segment assuming a constant burnup. 32 segments will be used, ranging from N1 at the bottom of the assembly to N32 at the top.

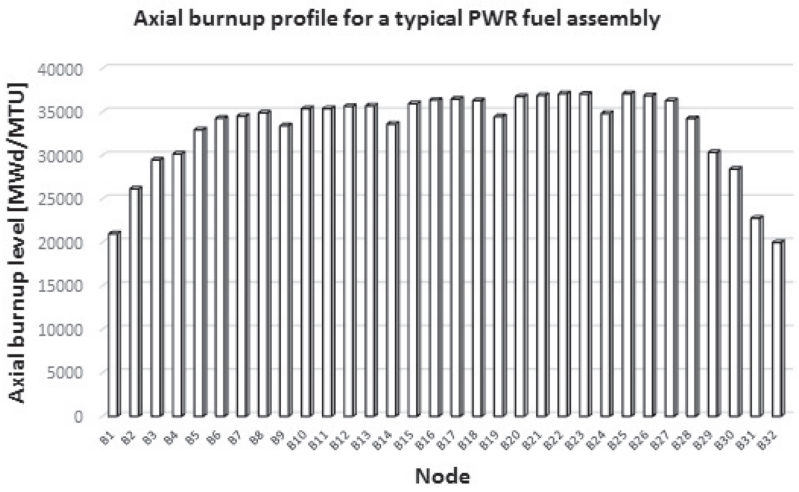

Figure 4.1: Axial burnup distribution for a fuel element in a PWR reactor [27].

Figure 4.2: Single fuel rod representation in KENO3D displaying the 32 segments division (not to scale).

4.1.1 Geometry.

The dimensions of both fuel element types are given in table 4.1. In figure 4.3 the distribution of the guide tubes for the insertion of the control rods can be observed.

Table 4.1: Specifications of the PWR fuel elements.

Reticule	16 x 16
Number of fuel pins	236
Number of guide tubes	20
Pin pitch	14.3 mm
Diameter of the fuel pellets	9.11 mm
External diameter of the pin	10.75 mm
Cladding thickness	0.725 mm
Cladding material	Zircaloy
External diameter of the guide tube	13.8 ± 0.03 mm
Internal diameter of the guide tube	12.4 mm
Material of the guide tube	Zircaloy
Mass of uranium by fuel element	473.2 kg ± 2%
Active length	3400 ± 15 mm

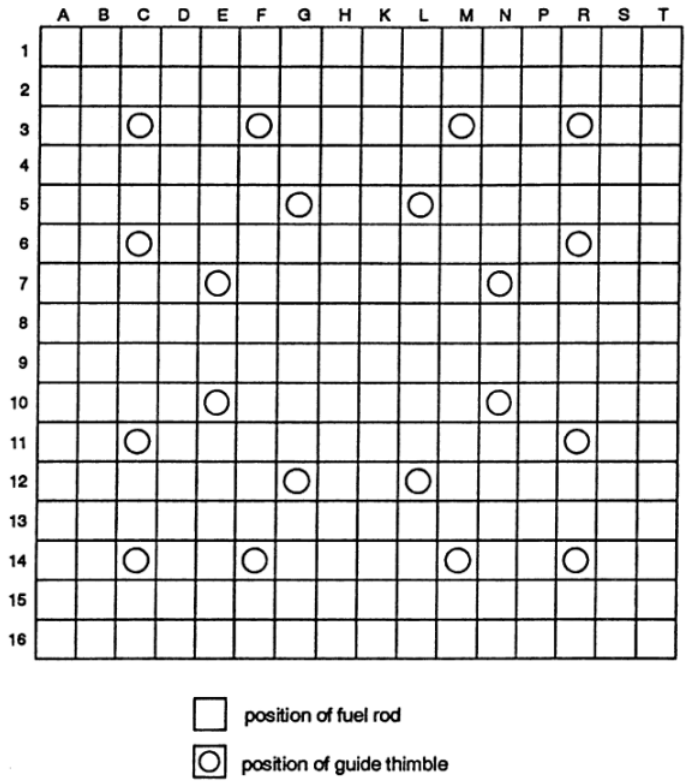

Figure 4.3: Rods distribution on the fuel elements.

4.1.2 Materials composition.

The fuel rods in each fuel element are modelled as shown in following Figure 4.4:

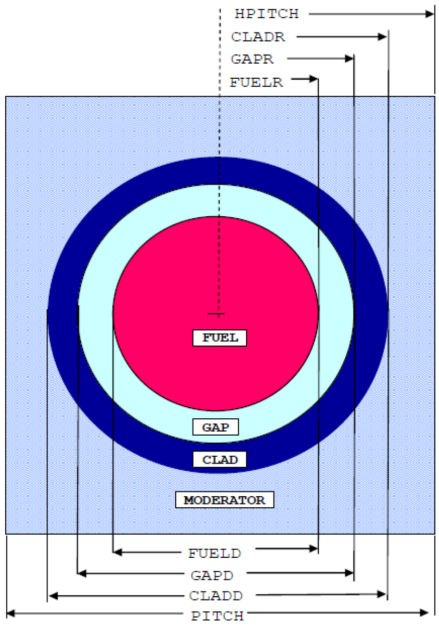

Figure 4.4: Top view of a fuel rod model.

The guide rods in the fuel elements have the same size as the fuel rods but are filled with water instead of "fuel" and "gap", allowing for the insertion of the control rods. As the later analysis assumes operation at maximum power during the 5 operating cycles, no control rods are used.

The fuel element components are made of the following materials (Table 4.2):

Table 4.2: Materials of the fuel element components.

Component	**Material**
FUEL	Uranium dioxide (UO_2) enriched at 5% of ^{235}U
CLAD	Zircaloy (table 4.3)
GAP	Helium
MODERATOR	Water

Table 4.3: Composition (% in volume) of the zircaloy used.

Element	**% in volume**
Zr	97.7155
Sn	1.5
Fe	0.4308
Cr	0.2042
O	0.14
Si	0.0095

4.1.3 Burnup data.

The first fuel element, type A, is calculated with a burnup of 51 $\frac{\text{GWd}}{\text{MTHM}}$, characteristic of the regular NPP operation over a 5-year period with the new 5% enriched fuel.

$$51\,\frac{\text{GWd}}{\text{MTHM}} \times \frac{10^9\,\text{W}}{1\,\text{GW}} \times \frac{1\,\text{MTHM}}{10^6\,\text{g HM}} \times \frac{1}{5\,\text{years} \times 365\,\text{days}} = 27.94521\,\frac{\text{W}}{\text{g HM}} \tag{4.1}$$

The second element, type B, is used to simulate a situation with a lower burnup and higher criticality, as less fissile material has been burned and it remains inside the fuel assembly. A burnup of 32.7 $\frac{\text{GWd}}{\text{MTHM}}$ (17.91866 $\frac{\text{W}}{\text{g HM}}$) is calculated, which could be the case of the least burned fuel assembly if the old NPP operation periods of about 3 years were used.

The following tables (Table 4.4, Table 4.5) show the burnup of each fuel element (F.E.) node ($\frac{\text{GWd}}{\text{MTHM}}$), and their corresponding specific power ($\frac{\text{W}}{\text{g HM}}$), unit used for the POLARIS input files.

Table 4.4: Burnup data of fuel elements type A and type B axial nodes ($\frac{\text{GWd}}{\text{MTHM}}$).

Axial nodes	**F.E. type** A	**F.E. type** B
N1	31.97	20.50
N2	40.55	26.00
N3	45.23	29.00
N4	46.79	30.00
N5	50.69	32.50
N6	52.56	33.70
N7	53.02	34.00
N8	54.58	35.00
N9	51.08	32.75
N10	54.74	35.10
N11	54.74	35.10
N12	54.90	35.20
N13	54.90	35.20
N14	51.15	32.80
N15	55.68	35.70
N16	56.14	36.00
N17	56.30	36.10
N18	55.83	35.80
N19	53.02	34.00
N20	56.30	36.10
N21	56.30	36.10
N22	56.46	36.20
N23	56.30	36.10
N24	53.80	34.50
N25	56.77	36.40
N26	56.46	36.20
N27	55.99	35.90
N28	53.02	34.00
N29	46.79	30.00
N30	43.67	28.00
N31	35.09	22.50
N32	31.19	20.00
Average burnup	**51.00**	**32.70**

Table 4.5: Specific power of fuel elements type A and type B axial nodes ($\frac{\mathrm{W}}{\mathrm{g\ HM}}$).

Axial nodes	**F.E. type** A	**F.E. type** B
N1	17.51833	11.23288
N2	22.21837	14.24658
N3	24.78203	15.89041
N4	25.63658	16.43836
N5	27.77296	17.80822
N6	28.79842	18.46575
N7	29.05479	18.63014
N8	29.90934	19.17808
N9	27.98660	17.94521
N10	29.99480	19.23288
N11	29.99480	19.23288
N12	30.08025	19.28767
N13	30.08025	19.28767
N14	28.02933	17.97260
N15	30.50753	19.56164
N16	30.76389	19.72603
N17	30.84935	19.78082
N18	30.59298	19.61644
N19	29.05479	18.63014
N20	30.84935	19.78082
N21	30.84935	19.78082
N22	30.93480	19.83562
N23	30.84935	19.78082
N24	29.48206	18.90411
N25	31.10571	19.94521
N26	30.93480	19.83562
N27	30.67844	19.67123
N28	29.05479	18.63014
N29	25.63658	16.43836
N30	23.92747	15.34247
N31	19.22743	12.32877
N32	17.09105	10.95890
Average specific power	**27.94521**	**17.91866**

4.2 Burnup calculations.

4.2.1 POLARIS input file.

This section will specify and explain the POLARIS commands necessary to perform the burn-up calculations. POLARIS has a very intuitive input file that allows the user to create mesh models with as few lines as possible. Many of the POLARIS cards or commands can be defined in an abbreviated form. All the cards or commands are described in the following figure 4.5:

card	*long command*	*short command(s)*
system	system	sys
geometry	geometry	geom
composition	composition	comp
property	property	prop
material	material	mat
burnup	bu or dbu	-
power	power	pow
options	option	opt
time	t or dt	-
state	state	-
branch block	branch	-
pin geometry component	pin	-
assembly pin map	pinmap	-
assembly channel	channel	-
assembly half gap	hgap	-
channel box	box	-
shield	shield	-
deplete	deplete	-
slab geometry component	slab	-
power basis materials	basis	-
assembly inserts	insert	-
assembly control elements water cross geometry displacement maps spatial meshing detector tallies operating histories restart cumulative burnup	control cross dxmap (dymap) mesh detector history bui (ti)	- - - - - - -

Figure 4.5: Polaris commands [26].

The first line of the input file (.inp) is written as:

```
=polaris_6.3
```

to start the POLARIS capability after executing SCALE. Right after, a title for the file is defined (16×16), together with the nuclear data library to be used in the calculation (v7-56, for the ENDF/B-VII.1 56-group neutron library).

```
title "16x16"
lib "v7-56"
```

The next cards defined are the system and geometry, a 16×16 PWR:

```
system PWR
geometry myPWR : ASSM 16 1.43 sym=SE
```

"myPWR" is an arbitrary assembly name. "ASSM" stands for assembly, "16" for the number of pins on each side of the assembly and "1.43" for the pin pitch, this is the distance between pin centers, measured in centimeters (cm). "SE" refers the assembly symmetry, south-east quarter, used in the pinmap card.

The distance between assemblies is fixed with the hgap card, measuring the half distance between them in cm:

```
hgap=0.12
```

To define custom materials, comp card is used. Two compositions are to be defined, the uranium dioxide and the zircaloy of the cladding:

```
comp uox_5 : UOX 5 refdens=10.5156
comp arbm-zirc : WT scale = PCT
    zr=97.7155
    sn=1.5
    fe=0.4308
    cr=0.2042
    o=0.14
    si=0.0095
```

"UOX" takes the data of uranium dioxide UO_2 from the nuclear data library, "5" fixes the amount of ^{235}U enrichment and "refdens" is the default density for the composition in g/cm^3. In the zircaloy composition, named arbitrarily "arbm-zirc", "WT scale = PCT" means the weight fraction of the composition shall be defined as a percentage of diferent elements with the values following it.

The next card, mat, links each component of the fuel element to their corresponding material. The five components of the table 4.2 are defined, plus the water coolant and the control rods:

```
mat FUEL.1 : uox_5
mat CLAD.1 : arbm-zirc dens=6.6 temp=591
mat GAP.1 : FILLGAS dens=1.E-3 temp=559
mat COOL.1 : WATER dens=0.73968 temp=559 boron=2200
mat MOD.1 : WATER dens=0.73968 temp=559
mat TUBE.1 : arbm-zirc dens=6.6 temp=559
mat CNTL.1   : AIC       dens=10.1586 temp=559
```

Note that "GAP.1", "COOL.1", "MOD.1" and "CNTL.1" use pre-defined default materials, not custom ones. "FILLGAS" is helium gas, "WATER" is light water and "AIC" is Ag-In-Cd control rod absorber material. The parameters that follow are the density of each material in g/cm^3 and temperature in K. The coolant WATER also contains 2200 parts per million (ppm) of initial boron solution. This property does not need to be the defined again in the moderator card.

The rods geometry is defined right after, labeled as "pins" in POLARIS:

```
pin 1 : 0.4555 0.465 0.5375
        : FUEL.1 GAP.1 CLAD.1
pin G : 0.62 0.69
        : COOL.1 TUBE.1
```

The pin geometry is constructed from the inside out, using circle zones defined by their interior radius (cm) and their corresponding material. The first pin defines the fuel rod and the second defines the guide tubes for the control rods insertion.

The layout of the pins inside the reactor core is defined with the pinmap card. As SE symmetry was used in the geometry card, the pinmap has the following form:

```
pinmap
1
1 1
1 1 1
1 G 1 1
1 1 1 1 1
1 1 G 1 1 G
1 1 1 1 1 1 1
1 1 1 1 1 1 1 1
```

In a similar way, we define the control rod pin "P" and its pin layout, in the same position as the guide tubes. The control card and RODLET argument is used to model the PWR-type rod cluster control assembly (RCCA):

```
pin P : 0.4902 0.5029 0.5601 0.63245 0.6731
        : CNTL.1 GAP.1 TUBE.1 COOL.2 CLAD.1
control Crod : RODLET

              -
              - -
              - - -
              - P - -
              - - - - -
              - - P - - P
              - - - - - - -
              - - - - - - - -
```

On the state card, property values such as density, void fraction, temperature or position of control rods are updated. One or more properties can be specified simultaneously. In this work, the state card will be used to define a specific history, so we will have to update the fuel temperature to 900 K and set the control rods outside of the core.

```
state FUEL : temp=900
      Crod : in=no
```

The specific operating cycle history parameters are defined with history card, that initiates a time-dependent calculation with user defined power history and time-dependent material or geometry properties. In these time dependant calculations, power will remain constant but the concentration of boron in the coolant will be decreased linearly, as in figure 3.12. Boron units are ppm, power unit is $\frac{\mathrm{W}}{\mathrm{g\,HM}}$ (specific power) and time steps are measured in days. Five operating cycles are defined, with a break of 30 days between each one to simulate refuelling time.

```
read history
%cycle 1
state COOL : boron= 2200 1937.5 1675 1412.5 1150 887.5 625 362.5 100
power 17.518330
t 0 25 50 100 150 200 250 300 365
power 0
t 395
%cycle 2
state COOL : boron= 2200 1937.5 1675 1412.5 1150 887.5 625 362.5 100
power 17.518330
t 398 425 450 500 550 600 650 700 760
power 0
t 790
```

```
%cycle 3
state COOL : boron= 2200 1937.5 1675 1412.5 1150 887.5 625 362.5 100
power 17.518330
t 793 825 850 900 950 1000 1050 1100 1155
power 0
t 1185
%cycle 4
state COOL : boron= 2200 1937.5 1675 1412.5 1150 887.5 625 362.5 100
power 17.518330
t 1188 1225 1250 1300 1350 1400 1450 1500 1550
power 0
t 1580
%cycle 5
state COOL : boron= 2200 1937.5 1675 1412.5 1150 887.5 625 362.5 100
power 17.518330
t 1583 1600 1650 1700 1750 1800 1850 1900 1945
end history
```

This is an example of the burnup of node N1 on the fuel element A (table **??**), with a specific power of 17.518330 $\frac{\mathrm{W}}{\mathrm{g\ HM}}$. The same calculation has been repeated a total of 2 fuel elements $\times$ 32 nodes = 64 times, changing the respective specific power for each one of the axial nodes.

Finally, some options for manipulating the solvers and output are added and the file is ended with the "end" command:

```
opt DEPL TrackingSet='Complete' Method='predictor_corrector'
opt KEFF NumPolar=6 NumAzim=2
opt ESSM NumPolar=1 NumAzim=1
opt PRINT XFile16=yes
end
```

- "DEPL": enables the addition of depletion nuclides to input materials. All nuclides available on the ORIGEN data library are included with the "TrackingSet='Complete'" parameter.
- "KEFF" and "ESSM": "NumPolar" defines the number of polar angles per octant, and "NumAzim" defines the number of azimuthal angles per octant.
- "PRINT": "XFile16" activates the output of a TRITON xfile016 nodal data library.

The final files are then run in the SCALE suite to perform the necessary depletion calculations.

4.3 Isotopic composition after burnup.

4.3.1 POLARIS output.

After running the POLARIS input files, a variety of output files with different extensions are generated:

- ".x16" is the TRITON xfile016 nodal data library, activated by the PRINT card in the previous section.
- ".t16" is a file with a few-group cross sections are archived to be used in subsequent core simulator calculations.
- ".idc" is a script file of the internal SCALE calculation.
- ".out" contains the primary output of the code execution and the overall summary of the calculations performed by POLARIS.
- ".msg" is the message log file.
- ".png" is an image of a quarter of the 2D reactor geometry that allows the visualization of the arrangement of fuel rods and guide tubes (Figure 4.6):

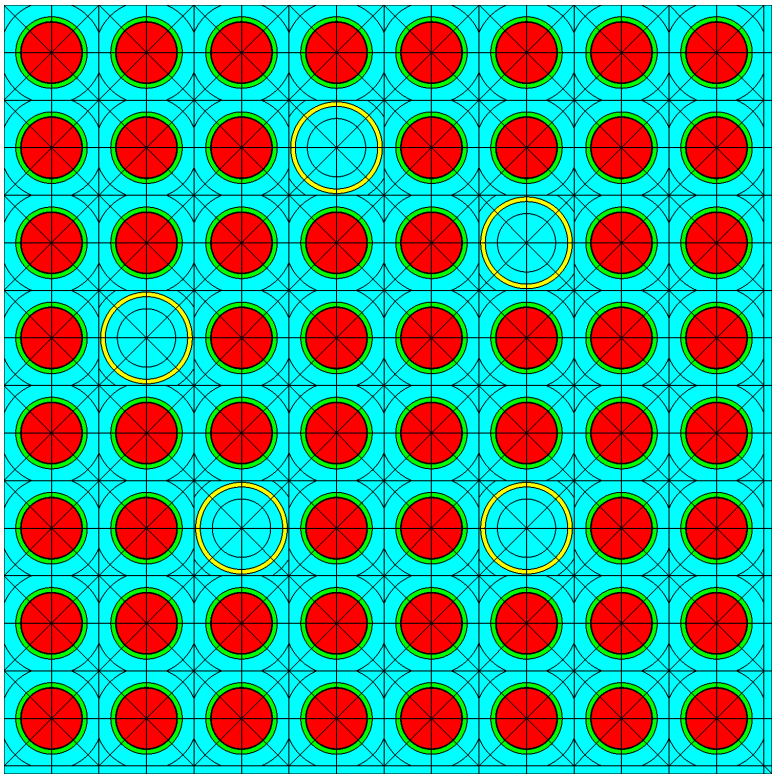

Figure 4.6: 2D lattice view of a quarter of the fuel element in the POLARIS ".png" output file.

- ".f71" is an ORIGEN binary concentration file. It is the main file for extracting the final calculated data.

4.3.2 Isotopes selection.

Although ORIGEN can track over 2000 nuclides and include all of them in the ".f71" output file, this much detail is not necessary. Many of those nuclides decay very rapidly and others are present in insufficient quantities to significantly impact k_{eff} calculations. The following criteria are recommended by [27] and [28]:

1. Include nuclides that significantly contribute to the absorption of thermal neutrons in spent fuel.
2. Include all fissile nuclides.
3. Only consider nuclides fixed in the fuel matrix, excluding volatile elements.
4. Ensure the predicted concentrations of selected nuclides in spent fuel can be verified by chemical assay measurements.

Criterion 2 requires the inclusion of ^{235}U,^{239}Pu and ^{241}Pu in the actinide set. Additionally, the guide [29] specifies that ^{135}Xe must not be included. Table 4.6 shows the 91 selected nuclides for the analysis:

Table 4.6: List of selected actinides and fission products.

Category	**Nuclides**
Actinides	^{234}U, ^{235}U, ^{236}U, ^{238}U, ^{237}Np, ^{238}Pu, ^{239}Pu, ^{240}Pu, ^{241}Pu, ^{242}Pu, ^{241}Am, ^{243}Am, ^{242}Cm, ^{243}Cm, ^{244}Cm
Fission Products	^{1}H, ^{10}B, ^{11}B, ^{14}N, ^{16}O, ^{83}Kr, ^{93}Nb, ^{94}Zr, ^{95}Mo, ^{99}Tc, ^{103}Rh, ^{105}Rh, ^{106}Ru, ^{109}Ag, ^{126}Sn, ^{135}I, ^{131}Xe, ^{133}Cs, ^{134}Cs, ^{135}Cs, ^{137}Cs, ^{143}Pr, ^{144}Ce, ^{143}Nd, ^{145}Nd, ^{146}Nd, ^{147}Nd, ^{147}Pm, ^{148}Pm, ^{149}Pm, ^{148}Nd, ^{147}Sm, ^{149}Sm, ^{150}Sm, ^{151}Sm, ^{152}Sm, ^{151}Eu, ^{153}Eu, ^{154}Eu, ^{155}Eu, ^{152}Gd, ^{154}Gd, ^{155}Gd, ^{156}Gd, ^{157}Gd, ^{158}Gd, ^{160}Gd, ^{91}Zr, ^{93}Zr, ^{95}Zr, ^{96}Zr, ^{95}Nb, ^{97}Mo, ^{98}Mo, ^{99}Mo, ^{100}Mo, ^{101}Ru, ^{102}Ru, ^{103}Ru, ^{104}Ru, ^{105}Pd, ^{107}Pd, ^{108}Pd, ^{113}Cd, ^{115}In, ^{127}I, ^{129}I, ^{133}Xe, ^{139}La, ^{140}Ba, ^{141}Ce, ^{142}Ce, ^{143}Ce, ^{141}Pr, ^{144}Nd, ^{153}Sm, ^{156}Eu

4.3.3 OBIWAN commands.

For the processing of the isotope data of the ".f71" file, the OBIWAN tool within the SCALE suite is used. The "obiwan view" command offers several options for formatting output which are specific to the file type being viewed, ".f71" in this case.

The full command used has the following form:

```
obiwan view -symbols=1 -units=gram -format=csv inputname.f71 >outputname.csv
```

With the option "-symbols" we choose between output numeric ids (1001) or symbols (H-1) of the nucleids. "1" is used for symbols, as it will facilitate further data processing.

With "-units", the units used for the output file are selected from the available list:

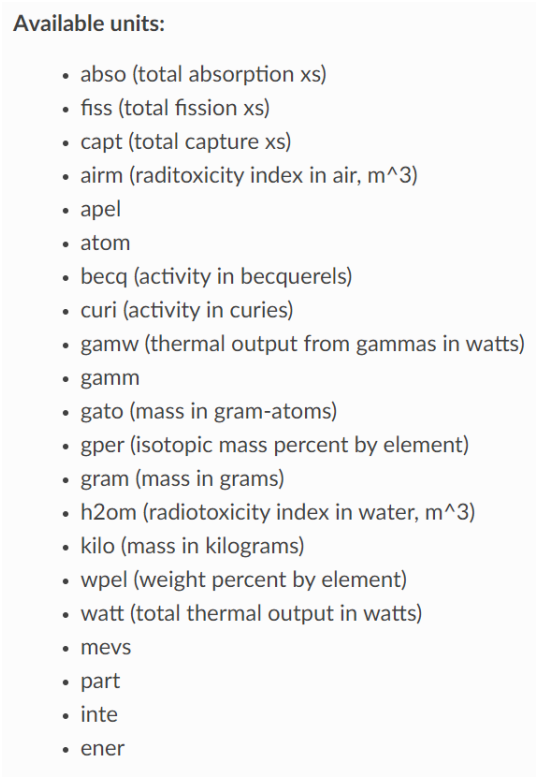

Figure 4.7: Available units for OBIWAN output [26].

Note that no unit for the composition of each isotope in weight percent exists, so the output cannot be translated into a KENO-VI composition input directly, requiring for the creation of the MATLAB© script developed in next section. The unit "gram" is used to perform the calculations of the weight percent by isotope for each relevant isotope from table 4.6 in the mentioned script.

With "-format" the target output fomat is fixed. For data processing with MATLAB©, the comma-separated values (CSV) format is used (.csv). CSV is a text file format that uses commas to separate values, and newlines to separate records.

Lastly, the names for the ".f71" input file and ".csv" output file are written with the greater than sign ">" between them.

4.3.4 MATLAB© script.

MATLAB© is a powerful tool used extensively for data analysis, visualization, and numerical computation. MATLAB© provides a wide array of functions for importing, processing, and exporting data. The full script developed for converting the POLARIS output data into KENO-VI composition input is shown in Annex 2.

The ".csv" file obtained with OBIWAN is composed by 2243 rows and 2990 columns. As detailed before, such level of detail is not relevant for the k_{eff} calculation. The data file is composed by

a total of 61 segmented cases, each one containing the 49 time steps of the history defined in the input file of POLARIS.

$$1\,\text{header column} + 61\,\text{cases} \times 49\,\text{time steps} = 2990\,\text{columns}$$

Of the 61 segmented cases, only the last one will be used, as it shows the overall total isotope composition of the fuel element. The data from the last time step is taken to calculate the input composition of KENO-VI.

The first 5 rows of the ".csv" file define the 'case' (61), 'step' (49 time steps for each case), 'time' (seconds), 'power' (specific power, $\frac{\text{W}}{\text{g HM}}$), 'flux' (neutron flux, $\text{cm}^{-2}\text{s}^{-1}$) and 'volume' of the statepoint calculation in progress. The remaining rows (2238) label the isotope, starting with the ORIGEN sublibrary definition (Table 4.7) and continuing with name symbols, as requested with the "obiwan view" command.

Table 4.7: ORIGEN sublibrary definition [26].

S	TY	DESCRIPTION
1	LT	light nuclides, typically the result of activation of common elements and structural materials, e.g. ^{16}O, ^{6}Li
2	AC	fissionable actinides and their immediate decay and activation products, e.g. ^{235}U, ^{239}Pu, ^{244}Cm
3	FP	fission products and their decay and activation products, e.g. ^{135}Te, ^{135}Cs, ^{135}Xe

The overall functioning of the script can be summarized in the following flowchart:

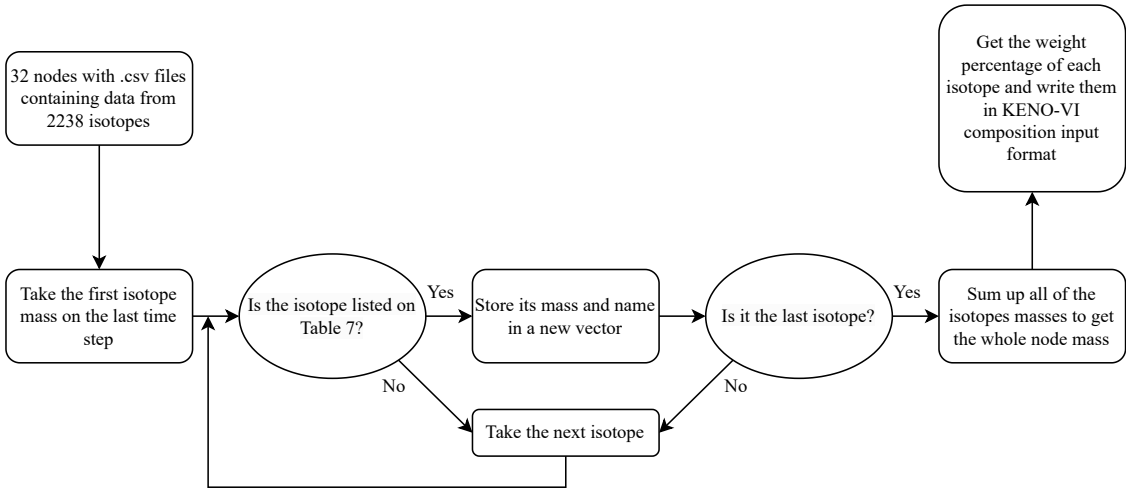

Figure 4.8: Flowchart of the POLARIS output processing data script.

4.3.5 MATLAB© and FULCRUM burnup analysis.

Some interesting data from the burnup can also be obtained and represented with MATLAB© and FULCRUM, the SCALE Graphical User Interface, such as the variation in weight percentage of the fuel assembly with each time step of the calculation (Figure 4.9). The data displayed in the following graphs corresponds to node N9 from fuel element type A, as it is the one with the closest burnup to the average.

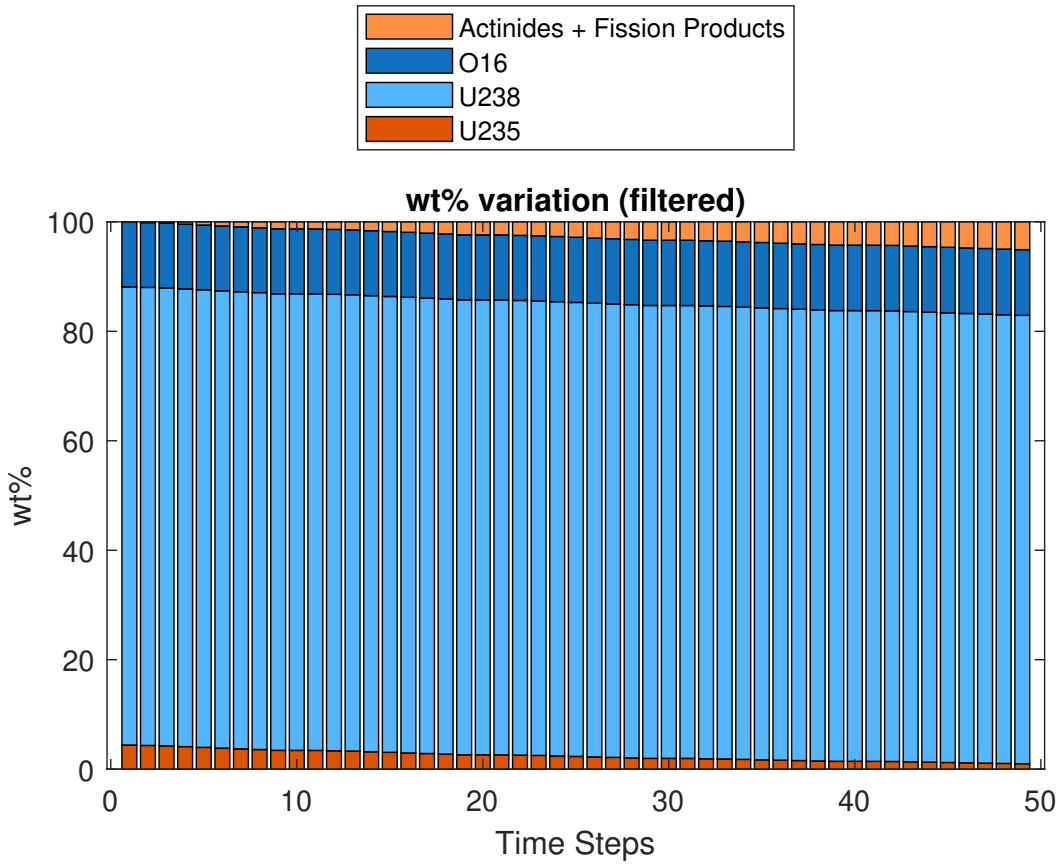

Figure 4.9: Weight percentage of the fuel element for each time step (F.E. type A, node N9).

After sorting the isotopes by final mass, the variations of all isotopes in Table 4.6 can be plotted over the 5-year period, as shown in Figure 4.10:

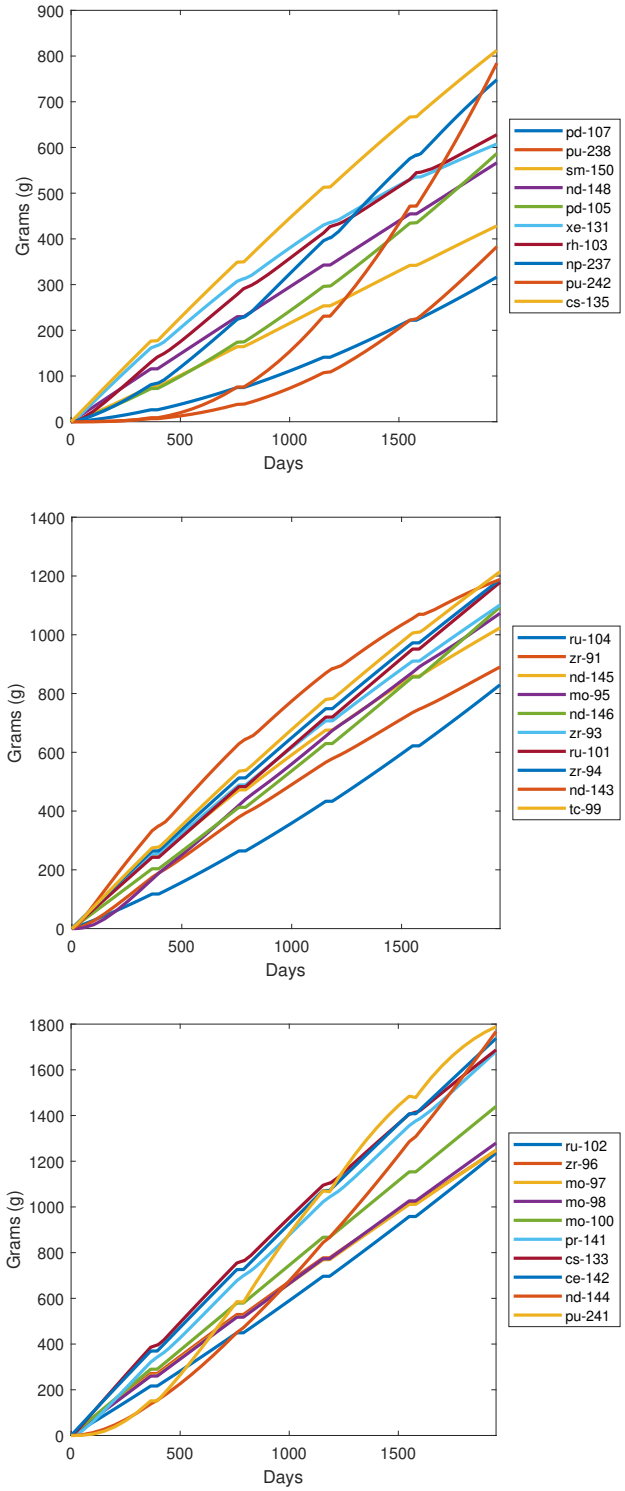

Figure 4.10: Mass over time of some of the selected isotopes (F.E. type *A*, node N9).

In plots with the days axis, the ”steps” in the corresponding 30-day periods where the reactor is shut down for refuelling can be appreciated. With these data, the same mass variations are also plotted in weight percentage over burnup to represent the evolution in a more convenient way in Figure 4.11.

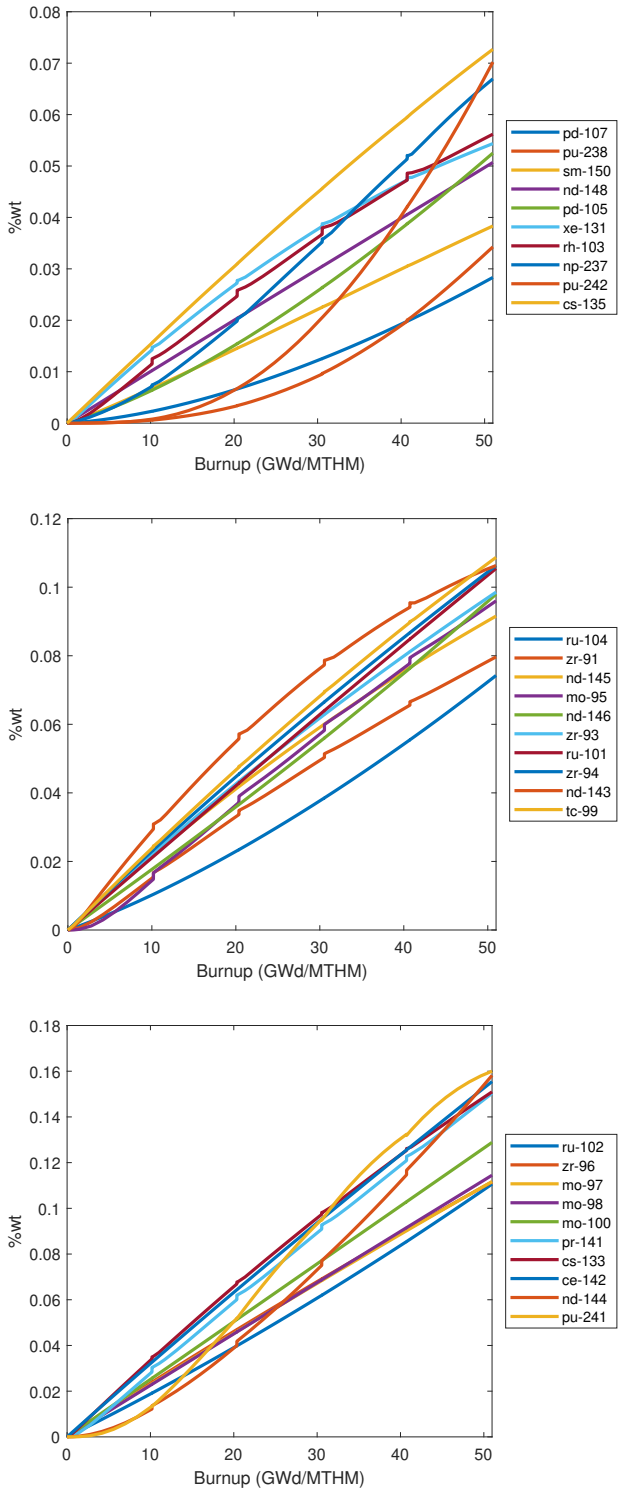

Figure 4.11: Weight percentage over burnup of some of the selected isotopes (F.E. type *A*, node N9).

This "step" effect can be highly appreciated with the most abundant isotope ^{235}U (excluding ^{16}O and ^{238}U, as their masses are out of scale and their variation is negligible) in Figure 4.12:

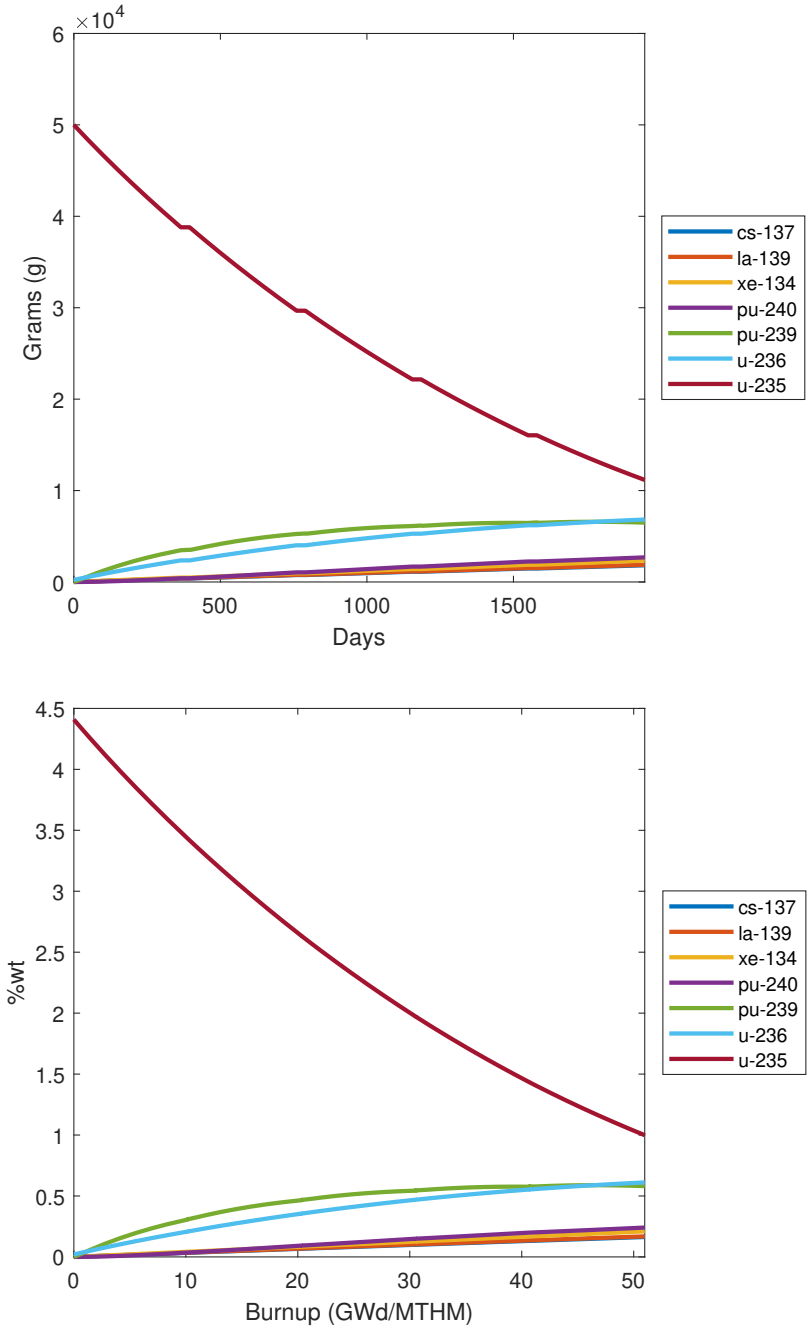

Figure 4.12: Mass over time and weight percentage over burnup of most abundant selected isotopes (F.E. type *A*, node N9).

Same variations can be compared with the plots generated by FULCRUM. Since ORIGEN does not extract weight percent data by isotope, the mass variation over time are the only comparable plots. Note that these 2D burnup calculations in POLARIS have no input of the reactor three-dimensional geometry, so no data from the total mass of uranium is taken into account. The grams shown are not total grams inside the reactor, but are based on calculations

per tonne of initial heavy metal. This is the reason why on day 0 there are 50000 grams (50 kg) of ^{235}U, which is 5% of the initial uranium (one tonne, 1000 kg).

The FULCRUM display always shows the total isotope data on the screen, with no option to hide it. In order to represent the graphs in a more readable way, the selected isotope data to be displayed have been extracted from the "Table" window and represented in the Microsoft Excel tool. As can be seen in Figure 4.12 and Figure 4.14, both the MATLAB© and FULCRUM representations of mass over time coincide:

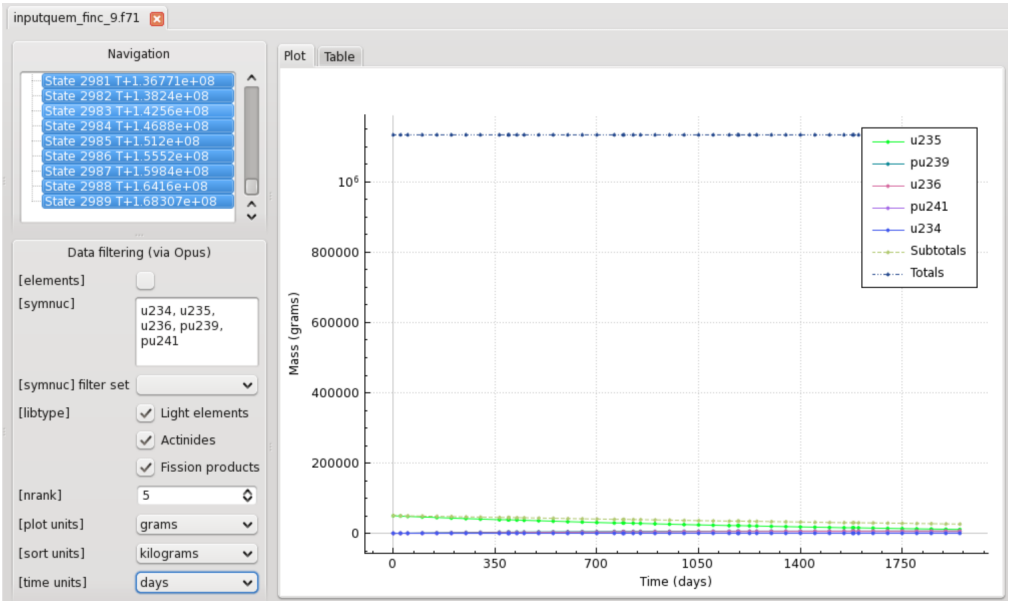

Figure 4.13: FULCRUM, the SCALE Graphical User Interface.

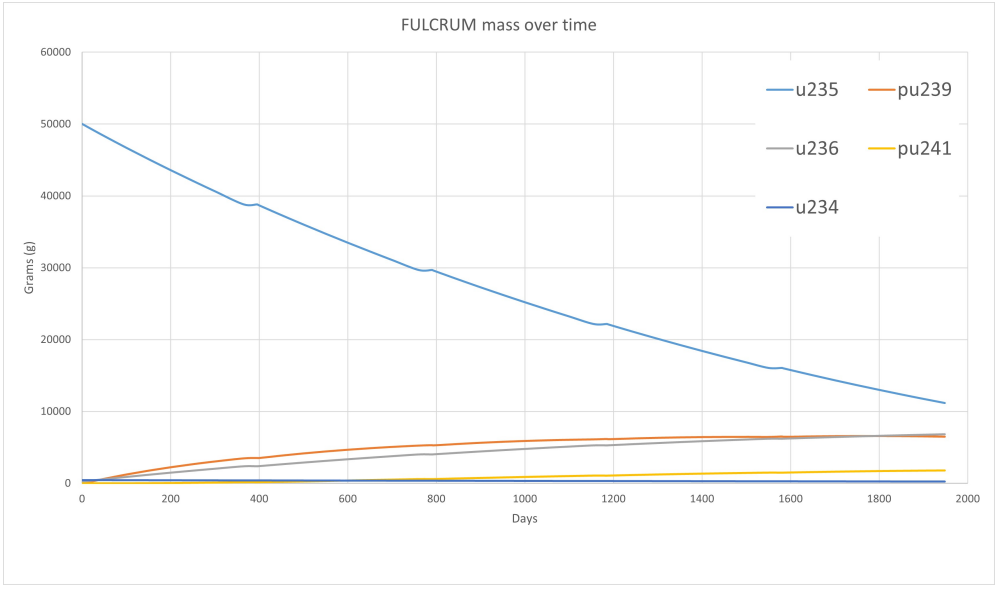

Figure 4.14: Plot generated in Microsoft Excel with data extracted from FULCRUM.

Another important burnup analysis is the mass defect. To calculate energy extracted from fuel element type A node 9 by mass defect, total mass at the end of the 5 years period can be substracted from total mass at the beginning of the first operating cycle:

$$1134197.171 - 1134133.362 = 63.809\,\mathrm{g}$$

$$E = m \cdot c^2 = 0.063809\,\mathrm{kg} \cdot (299792458\frac{\mathrm{m}}{\mathrm{s}})^2 =$$

$$= 5.73 \times 10^{15}\,\mathrm{J} = 5.73 \times 10^{9}\,\mathrm{MJ}$$

This energy can be compared with the result of the thermal energy calculation obtained from the specific power used during the 5 years period:

$$\text{Specific power} = \ 27.9866\,\frac{\mathrm{W}}{\mathrm{g\ HM}}$$

$$27.9866\,\frac{\mathrm{W}}{\mathrm{g\ HM}} \times \frac{1\,\mathrm{MW}}{10^6\,\mathrm{W}} \times \frac{10^6\,\mathrm{g\ HM}}{1\,\mathrm{MTHM}} \times 1\,\mathrm{MTHM} = 27.9866\,\mathrm{MW}$$

$$27.9866\,\mathrm{MW} \times \ 5\ \mathrm{years} \times \ 365\ \mathrm{days} \times \ 24\ \mathrm{hours} \times \ 60\ \mathrm{min.} \times \ 60\ \mathrm{sec.} = 4.41 \times 10^{9}\,\mathrm{MJ}$$

This shows that the thermal energy generated by the fuel element corresponds to $\approx 77\%$ of the energy generated by fission.

$$\frac{4.41 \times 10^9}{5.73 \times 10^9} \times 100 = 76.95\,\%$$

This is a quite reasonable result since effects such as neutrino losses or transmutations of intermediate elements have to be taken into account for a more accurate result.

The last significant plot is the weight percentage of ^{235}U for each node of a fuel element, showing the inverse form of the generated power graph sine-wave distribution, displaying the fact that the least burnt parts of the fuel element are located at its ends:

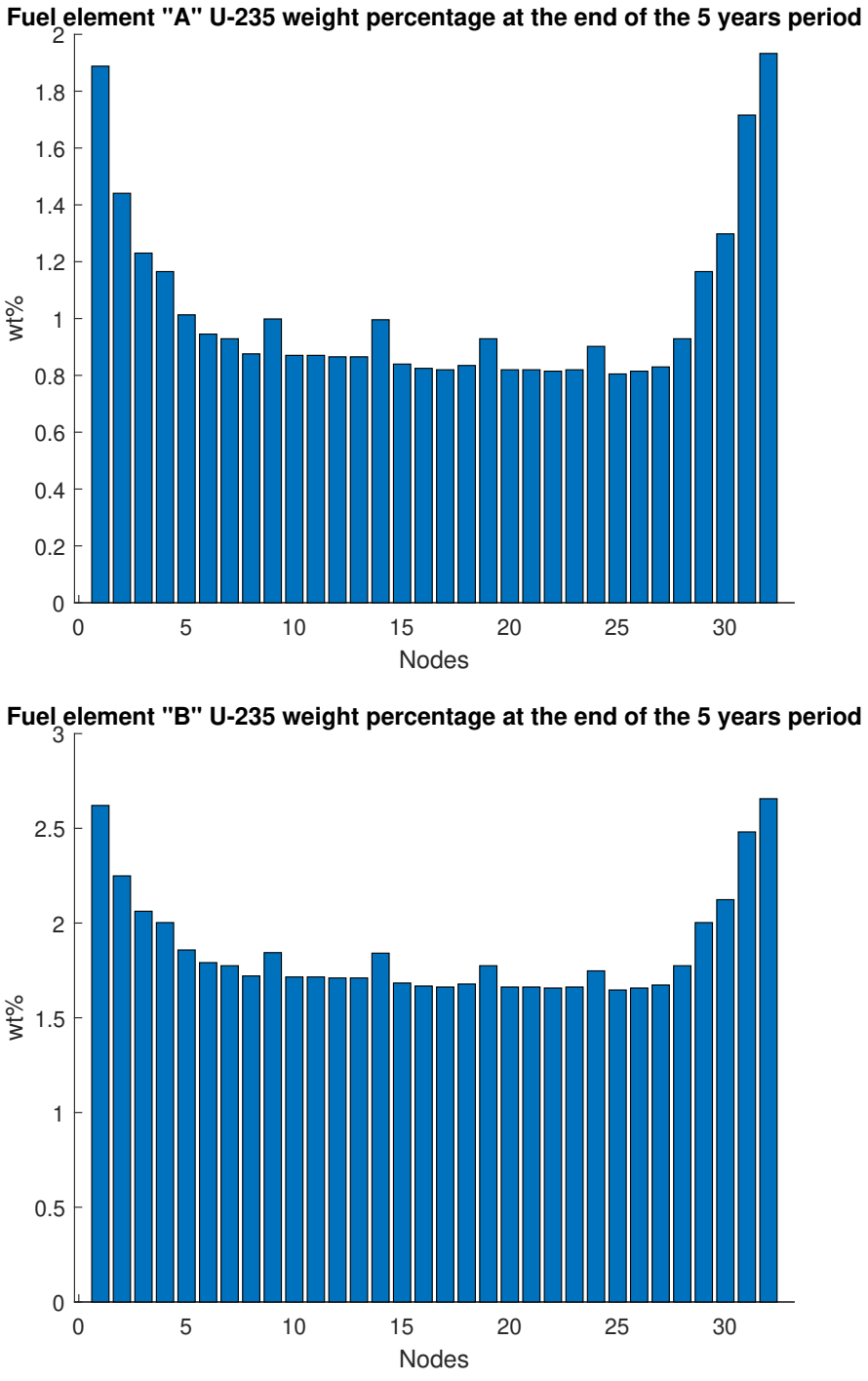

Figure 4.15: Distribution of ^{235}U in each fuel element type at the end of the 5 years period calculated in POLARIS.

As expected, the less burnup in fuel element type B means more fissile ^{235}U remains in it. This also means that its criticality is higher.

4.4 Criticality analysis.

4.4.1 Spent fuel pool geometry.

In order to be able to calculate the criticality of the fuel assemblies within the spent fuel pool, the geometry of the pool and its dimensions have to be represented. As previously mentioned, the original construction pool was divided into two regions. This work focuses on region II, where the storage of the completely burned fuel is expected.

The region II of the spent fuel pool, composed by barriers of borated steel in a chess-like matrix, can be modelled from a basic, or reference cell, with boundary conditions of specular reflection on the XY axes as follows (Figure 4.16):

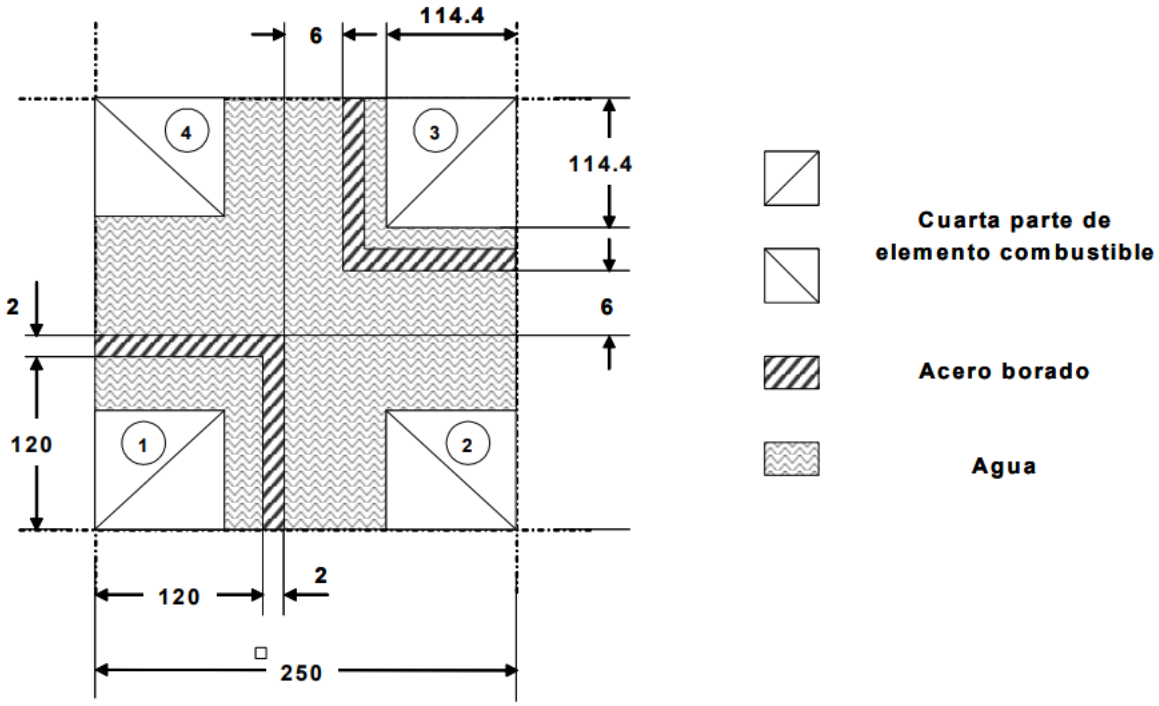

Figure 4.16: Outline of the reference cell model.

With this geometry 3 cases will be calculated with KENO-VI. In the first and the second one, all of the fuel elements will be respectively take the compositions of fuel elements type A and B. In the third case, the fuel elements protected by the borated steel will have the composition of the fuel element type B, as it is the most critical one. The rest of the fuel elements will take the fuel element type A composition. In all 3 cases no credit for soluble boron is taken, this means that in the assumed calculations the pool water does not contain any boron.

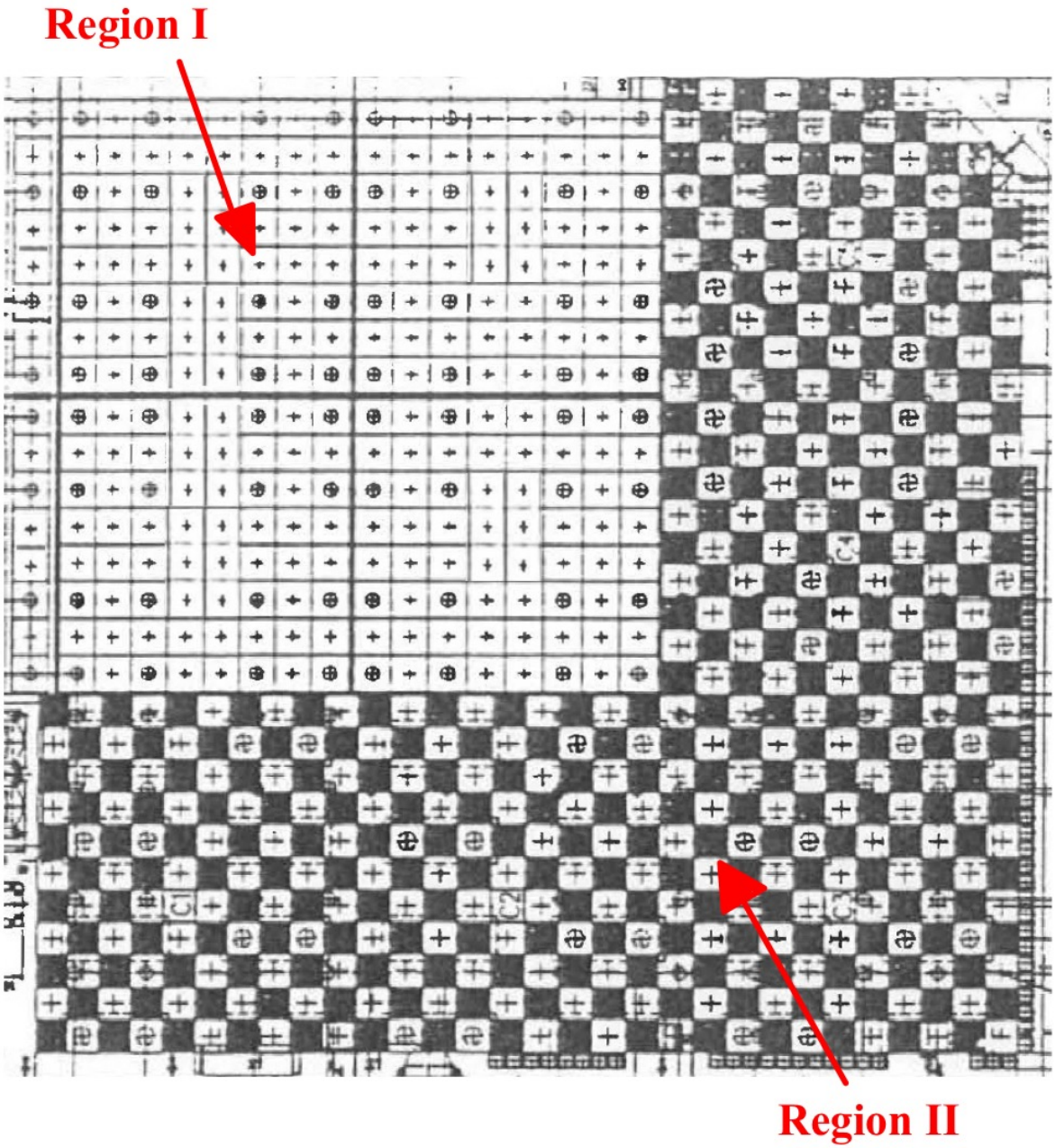

Figure 4.17: Region I and II of the spent fuel storage pool.

4.4.2 KENO-VI input file.

This section will specify and explain the KENO input data necessary to perform the criticality calculations.

Type of data	Keyword
Parameters	`PARAMETER` , `PARA` or `PARM`
Geometry	`GEOMETRY` , `GEOM`
Biasing	`BIAS`
Boundary conditions	`BOUNDS` , `BOUN` or `BNDS`
Start	`START` , `STAR` or `STRT`
Energy	`ENERGY` or `ENER`
Array (unit orientation)	`ARRAY` or `ARRA`
Extra 1-D cross sections	`X1DS`
Cross section mixing table[a]	`MIXT` or `MIX`
Plot[a]	`PLOT` or `PLT` or `PICT`
Volumes	`VOLUME`
Grid geometry	`GRIDGEOMETRY` , `GRIDGEOM` , or `GRID`
Reactions	`REACTION` , `REAC`

[a] MIX and PLT must include a trailing blank, which is considered part of the keyword.

Figure 4.18: KENO types of input data.

```
=sequence_identifier parm=(parm_options)
problem title

' ----- XSProc data
' cross section library name (REQUIRED)
ce_v7.1

' List of material specifications in standard SCALE format (REQUIRED)
read composition
...
end composition

' Specify data for resonance processing (OPTIONAL)
read celldata
...
end celldata

' ---- New CSAS sequence data blocks

' Used to define energy bounds and grid geometries for
' the tallies defined in tallies data block
' (REQUIRED if tallies data block exists)
read definitions
...
end definitions

' Used to define tallies in a more robust way (OPTIONAL)
read tallies
...
end tallies

' ---- KENO transport data
' Specify the problem geometry (REQUIRED)
read geometry
...
end geometry

' Other input data blocks (OPTIONAL)
```

Figure 4.19: Typical CSAS sequence input.

As KENO is run as part of a CSAS sequence, the corresponding input is define. This section describes the input data required for the CSAS with KENO transport codes. The keyword "com=" signals that a comment is to be read. First of all, the choose of the sequence identifier is defined:

```
=csas6 parm=centrm
```

The parameter centrm is used to process all fissionable cells.

A title for the file is written in the next line and then the cross section library name is specified. The same library used in POLARIS is applied:

```
ce_v7_endf
```

Now, the output composition generated with the MATLAB© script for each one of the 32 ".csv" files in a fuel element inside the "composition" list:

```
read composition
 b-10    1  den=10.5124    1.055055e-17    293    end
 b-11    1  den=10.5124    4.663367e-13    293    end
 ...
 zr-96   32  den=10.5124    7.040970e-04    293    end
```

The first digit "1" defines the identifier of the composition. As there are 32 axial nodes, 32 different compositions are used to define the nodes isotopes concentration. "den" defines the density of the composition in g/cm^3. The standard density of the UO_2 is used, as the difference between node segments is neglictible. Next value is the weight percentage of each isotope in the composition. The last number reflects the temperature in K. The pool is supposed to operate at 20 degrees Celsius, 293 degrees Kelvin.

The next composition defined is the zircaloy, in the same proportion as the one defined in POLARIS:

```
zr          33 0.97785 293   end
sn          33 0.01170 293   end
fe          33 0.00167 293   end
cr          33 0.00091 293   end
o           33 0.00787 293   end
```

In a similar way, the borated steel from the region II of the pool is defined:

```
wtpt-steelb     99  7.647  4
                                5000 1.7
                                24000 17.694
                                28000 9.83
                                26000 70.776
                          1 293   end
```

The first value "99" is the composition identifier. The next one is the steel density in g/cm^3 and "4" are the elements that the steel is made of. 5, 24, 28 and 26 are the atomic numbers of Boron,

Chromium, Nickel and Iron, and the values represent each element weight percentage. The last number is used again to define the temperature in K.

The last part of the composition is composed by the already defined materials in the library: water, helium and stainless steel:

```
 h2o          65 1 293 end
 he           66 1 293 end
 ss316        67 1 293 end
end composition
```

The next part specifies data for resonance processing with the "celldata" block, using the materials and geometry of the fuel element. This can be done for just one mixture number:

```
read celldata
  latticecell squarepitch fuelr=0.4555  1 gapr=0.465 0 cladr=0.5375 33 ...
    ... hpitch=0.715 65 end
end celldata
```

Additional parameters for the KENO transport calculation are defined in the next block "parameter":

```
read parameter
 gen=805
 npg=600
 htm=yes
 nb8=700
end parameter
```

- "gen" = number of generations to be run.
- "npg" = number of neutrons per generation.
- "htm" = activate the output of a html summary file.
- "nb8" = number of blocks allocated for the first direct-access unit

The geometry can be defined with the "geometry" block. First, the 32 segments of the fuel rods in the fuel element are defined:

```
read geometry
unit 1
 cylinder 1   0.4555  10.671875        0
 cylinder 2    0.465  10.671875        0
 cylinder 3   0.5375  10.671875        0
 cuboid 4    0.715   -0.715    0.715   -0.715  10.671875        0
 media 1 1 1 vol=1641.645453
 media 66 1 2 -1 vol=69.191063
 media 33 1 3 -2 -1 vol=575.075669
 media 65 1 4 -3 -2 -1 vol=2864.296271
 boundary 4
```

The first part of cylinders defines the geometry properties of the rods, in a similar way than were defined in POLARIS, from the inner to the exterior radius in cm. The cuboid of water of $0.715 + 0.715 = 1.43$ cm represents the distance between each fuel rod, known as pitch. The first 2 values specify the X axis length and the 2 next ones specify the Y axis length. The material of each layer is assigned in the next "media" rows.

The unit 33 are the spring clads located at the bottom and upper ends of the fuel rods and made of stainless steel:

```
unit 33
 com='spring clad'
 cylinder          1  0.4555  10.625  0
 cylinder          2  0.465   10.625  0
 cylinder          3  0.5375  10.625  0
 cuboid                4  0.715  -0.715  0.715  -0.715  10.625  0
 media 67 1 1
 media 66 1 2 -1
 media 33 1 3 -2 -1
 media 65 1 4 -3 -2 -1
 boundary 4
```

The guide tubes are defined the same way and filled with water in their inner hole:

```
unit 34
 com='guide tube'
 cylinder         1  0.62   10.625  0
 cylinder         2  0.69   10.625  0
 cuboid          3  0.715  -0.715  0.715  -0.715  10.625  0
 media 65 1 1
 media 33 1 2 -1
 media 65 1 3 -2 -1
 boundary 3
```

The next defined units are the fuel rods in their total length, containing an array of the 32 node segments plus the spring clads at the end of the rods. The total rod length is 340cm, specified in a symmetry in the Z direction as 170cm. The length of each node is therefore $340/32 = 10.625$ cm. The same node length is used at the ends to accommodate for the spring clads. Unit 35 will contain the fuel rods and unit 36 the guide tubes:

```
unit 35
cuboid 1    0.715   -0.715    0.715   -0.715   180.625  -180.625
array 1 1  place 1 1 1 0 0 -180.625
boundary 1
unit 36
cuboid 1    0.715   -0.715    0.715   -0.715   180.625  -180.625
array 2 1  place 1 1 1 0 0 -180.625
boundary 1
```

Now the fuel elements have to be placed in their respective positions. The 4 quarters of figure 4.16 are defined, each one with a different array that will be composed of the 8x8 quarter geometry of each corresponding fuel element.

```
unit 37
com="quarter 1"
 cuboid 1     5.72    -5.72     5.72    -5.72   180.625  -180.625
 array 6 1  place 1 1 1 -5.005 -5.005 0
 boundary 1
unit 38
com="quarter 2"
 cuboid 1     5.72    -5.72     5.72    -5.72   180.625  -180.625
 array 5 1  place 1 1 1 -5.005 -5.005 0
 boundary 1
unit 39
com="quarter 3"
 cuboid 1     5.72    -5.72     5.72    -5.72   180.625  -180.625
 array 3 1  place 1 1 1 -5.005 -5.005 0
 boundary 1
unit 40
com="quarter 4"
 cuboid 1     5.72    -5.72     5.72    -5.72   180.625  -180.625
 array 4 1  place 1 1 1 -5.005 -5.005 0
 boundary 1
```

In order to finish the geometry components, the horizontal and vertical parts of the borated steel walls are defined:

```
unit 41
com="x borated steel part"
 cuboid 1      6.1     -6.1      0.1     -0.1   180.625  -180.625
 media 99 1 1 vol=1666.52
 boundary 1
unit 42
com="y borated steel part"
 cuboid 1      0.1     -0.1  5.999999  -5.999999   180.625  -180.625
 media 99 1 1 vol=1639.2
 boundary 1
```

The last part of the geometry is combining all of the components. This is called the ”global unit”. A water cuboid is made and the 4 quarters of fuel elements and the borated steel parts are inserted in their respective place. 30cm of water are added on each end of the assembly to account for the boundary conditions in the Z axis:

```
global unit 43
 cuboid 1     12.5    -12.5     12.5    -12.5   210.625  -210.625
 hole 40   origin  x=-6.78 y=6.78 z=0
 hole 39   origin  x=6.78 y=6.78 z=0
 hole 38   origin  x=6.78 y=-6.78 z=0
 hole 37   origin  x=-6.78 y=-6.78 z=0
 hole 41   origin  x=-6.4 y=-0.4 z=0
 hole 41   origin  x=6.4 y=0.4 z=0
 hole 42   origin  x=-0.4 y=-6.5 z=0
 hole 42   origin  x=0.4 y=6.5 z=0
 media 65 1 1 vol=31358.45
 boundary 1
end geometry
```

After defining the geometry, the composition of the arrays for the fuel rods, guide tubes and the 4 quarters of the fuel elements containing them are defined:

```
read array
com="fuel rod"
ara=1 nux=1 nuy=1 nuz=34 typ=square
 fill
   33
   1
   2
   3
   4
   5
   6
   7
   8
   9
   10
   11
   12
   13
   14
   15
   16
   17
   18
   19
   20
```

```
   21
   22
   23
   24
   25
   26
   27
   28
   29
   30
   31
   32
   33  end fill
com="guide tube"
ara=2 nux=1 nuy=1 nuz=34 typ=square
 fill
   34
   34
   34
   34
   34
   34
   34
   34
   34
   34
   34
   34
   34
   34
   34
   34
   34
   34
   34
   34
   34
   34
   34
   34
   34
   34
   34
   34
   34
   34
   34
```

```
           34
           34
           34  end fill
com="quarter 3"
ara=3 nux=8 nuy=8 nuz=1 typ=square
fill
   35   35   35   35   35   35   35   35
   35   35   35   36   35   35   35   35
   35   35   35   35   35   36   35   35
   35   36   35   35   35   35   35   35
   35   35   35   35   35   35   35   35
   35   35   36   35   35   36   35   35
   35   35   35   35   35   35   35   35
   35   35   35   35   35   35   35   35  end fill
com="quarter 4"
ara=4 nux=8 nuy=8 nuz=1 typ=square
 fill
   35   35   35   35   35   35   35   35
   35   35   35   35   36   35   35   35
   35   35   36   35   35   35   35   35
   35   35   35   35   35   35   36   35
   35   35   35   35   35   35   35   35
   35   35   36   35   35   36   35   35
   35   35   35   35   35   35   35   35
   35   35   35   35   35   35   35   35  end fill
com="quarter 2"
ara=5 nux=8 nuy=8 nuz=1 typ=square
 fill
   35   35   35   35   35   35   35   35
   35   35   35   35   35   35   35   35
   35   35   36   35   35   36   35   35
   35   35   35   35   35   35   35   35
   35   36   35   35   35   35   35   35
   35   35   35   35   35   36   35   35
   35   35   35   36   35   35   35   35
   35   35   35   35   35   35   35   35  end fill
```

```
com="quarter 1"
ara=6 nux=8 nuy=8 nuz=1 typ=square
 fill
   35   35   35   35   35   35   35   35
   35   35   35   35   35   35   35   35
   35   35   36   35   35   36   35   35
   35   35   35   35   35   35   35   35
   35   35   35   35   35   35   36   35
   35   35   36   35   35   35   35   35
   35   35   35   35   36   35   35   35
   35   35   35   35   35   35   35   35  end fill
end array
```

Lastly, the boundary conditions for the XY plane symmetry are defined and the file is ended and ready to be run:

```
read bnds
 +xb=mirror
 -xb=mirror
 +yb=mirror
 -yb=mirror
 +zb=vacuum
 -zb=vacuum
  end bnds
end data
end
```

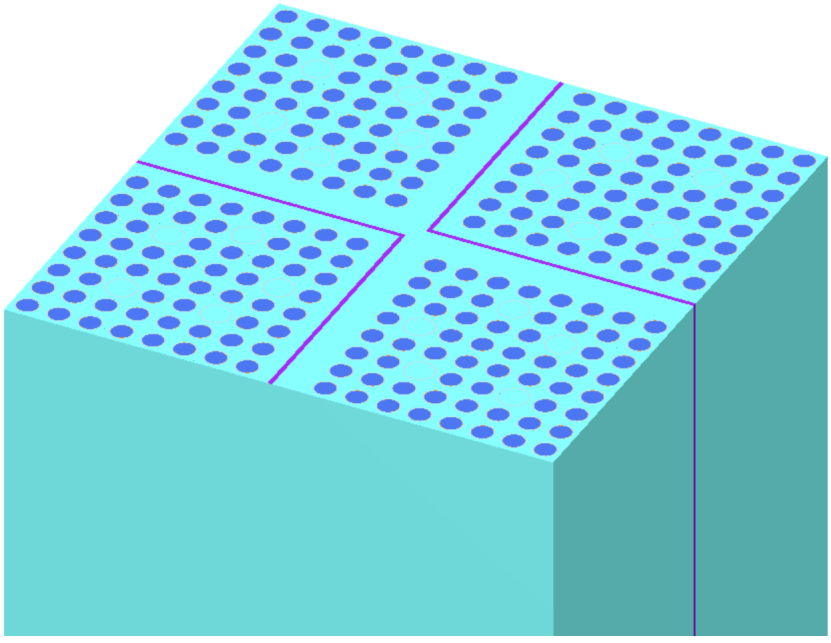

Figure 4.20: KENO 3D visualization of the region II pool assembly cross-section.

4.5 Results.

As mentioned above, 3 different pool storage scenarios have been calculated. An overview of them is shown in the figure 4.21 below:

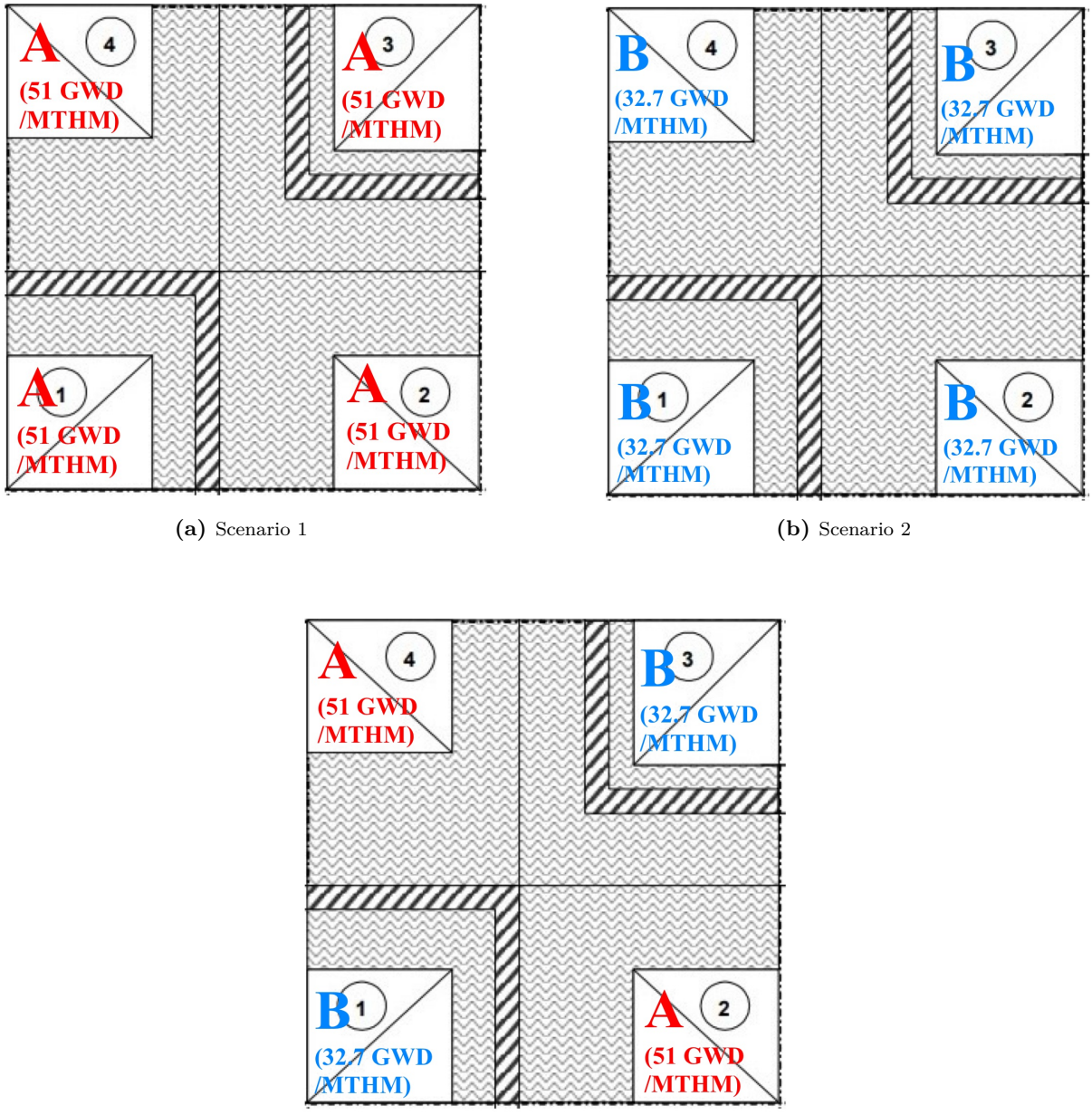

(a) Scenario 1

(b) Scenario 2

(c) Scenario 3

Figure 4.21: Overview of the 3 scenarios calculated in the spent fuel pool.

These scenarios, without taking any credit for the soluble boron in the water, have produced the following results (Table 4.8):

Table 4.8: k_{eff} and k_{eff} (95/95) values.

	k_{eff}	σ	k_{eff} (95/95)
Scenario 1	0.9178	0.0013	0.9207
Scenario 2	1.0184	0.0011	1.0209
Scenario 3	0.9543	0.0011	0.9568

Credit for soluble boron must be taken for scenarios 2 and 3, as their value exceeds the guide threshold of 0.95. The amount of boron, for instance, 500 ppm can be added in the KENO-VI composition as follows:

```
h2o         65 0.9995 293 end
boron       65 0.0005 293 end
```

The calculations of the mentioned scenarios taking credit for soluble boron have given the results shown in Table 4.9 and Table 4.10. The k_{eff} (95/95) value is obtained with Eq. 3.19.

Table 4.9: k_{eff} (95/95) in Scenario 2 taking credit for soluble boron.

Boron (ppm)	k_{eff}	σ	k_{eff} (95/95)
2200	0.6324	0.0013	0.6387
2100	0.6428	0.0015	0.6494
2000	0.6521	0.0013	0.6584
1900	0.6620	0.0011	0.6680
1800	0.6735	0.0012	0.6796
1700	0.6856	0.0012	0.6917
1600	0.6972	0.0011	0.7032
1500	0.7088	0.0011	0.7148
1400	0.7219	0.0012	0.7280
1300	0.7397	0.0014	0.7462
1200	0.7525	0.0012	0.7586
1100	0.7703	0.0011	0.7763
1000	0.7831	0.0012	0.7892
900	0.8007	0.0012	0.8068
800	0.8211	0.0012	0.8272
700	0.8387	0.0011	0.8447
600	0.8604	0.0013	0.8667
500	0.8859	0.0014	0.8924
400	0.9051	0.0011	0.9111
300	0.9315	0.0012	0.9376
200	0.9577	0.0013	0.9640
100	0.9881	0.0013	0.9944
0	1.0184	0.0011	1.0244

Table 4.10: k_{eff} (95/95) in Scenario 3 taking credit for soluble boron.

Boron (ppm)	k_{eff}	σ	k_{eff} (95/95)
2200	0.5896	0.0012	0.5957
2100	0.6007	0.0011	0.6067
2000	0.6079	0.0012	0.6140
1900	0.6189	0.0012	0.6250
1800	0.6305	0.0011	0.6365
1700	0.6409	0.0012	0.6470
1600	0.6488	0.001	0.6546
1500	0.6631	0.0011	0.6691
1400	0.6771	0.0013	0.6834
1300	0.6891	0.0011	0.6951
1200	0.7028	0.0011	0.7088
1100	0.7172	0.0013	0.7235
1000	0.7312	0.0011	0.7372
900	0.7475	0.0011	0.7535
800	0.7624	0.0012	0.7685
700	0.7849	0.0013	0.7912
600	0.8048	0.0011	0.8108
500	0.8256	0.0011	0.8316
400	0.85	0.0013	0.8563
300	0.8705	0.0012	0.8766
200	0.8949	0.0011	0.9009
100	0.9275	0.0011	0.9335
0	0.9543	0.0011	0.9603

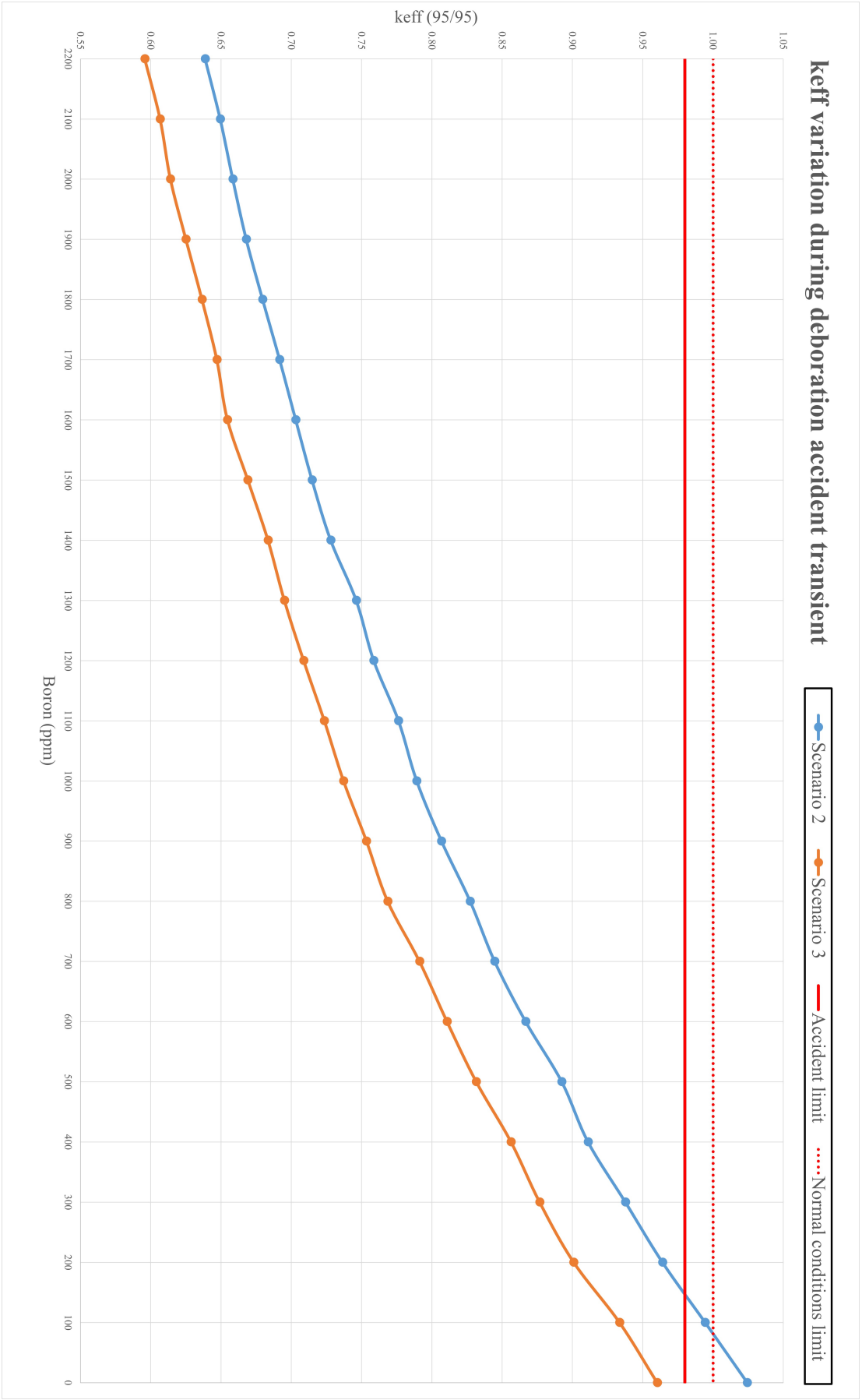

Figure 4.22: k_{eff} (95/95) variation during a deboration transient accident.

Chapter 5

Conclusions and future perspectives

In this work, the burnup of 2 PWR fuel elements with a 5% ^{235}U enrichment during 5 operating cycles of 1 year has been calculated with POLARIS code, taking into account their heterogeneity in the power distribution along their longitudinal axis, represented with 32 axial nodes with different specific power. After doing so, the data obtained has been analyzed with MATLAB© and the isotopic composition of each axial node has been extracted. These nodal compositions have been incorporated in the model of the spent fuel pool in KENO-VI code in order to proceed with the Criticality calculation in three different scenarios.

This new approach to Criticality calculation using burnup credit methodology has made it possible to obtain results that are closer to the reality of NPPs spent fuel, while at the same time making it possible to verify compliance with current nuclear safety and radiation protection standards. The results obtained show that previous approach to Criticality analysis, where no credit was taken for soluble boron, is not applicable to fuel enriched with 5% ^{235}U anymore.

Taking no credit for soluble boron, scenario 1 is compliant, but both scenarios 2 and 3 k_{eff} (95/95) values are above the 0.95 threshold. After taking credit for soluble boron, scenario 2 still does not comply in any case since its k_{eff} (95/95) value with unborated water is higher than 1. In order to be able to store type B fuel assemblies, scenario 3 must be used. The minimum allowable amount of boron to ensure a Criticality of less than 0.98 in this scenario with accident conditions is in fact 0 ppm, showing that its storage is safe under both normal and accident conditions.

It is worth mentioning that the case of a complete deboration accident in a spent fuel pool has very low probability and has never happened in nuclear power history. Current pools are always monitored and have systems to regulate the amount of boron present even in accidental cases. However, the remote possibility of such a transient must always be taken into account for safety analysis.

The work carried out has provided first-hand knowledge of the analysis and calculation processes in the nuclear industry with state-of-the-art codes. In addition, the calculation method developed in this work can be used in the future to optimize both the burnup and the fuel unloading patterns of the PWR nuclear reactor, taking into account the restrictions established by Criticality of the spent fuel pool.

Part II

Bibliography

[1] H. Ritchie, P. Rosado, and M. Roser, *Energy production and consumption*, 2020. [Online]. Available: https://ourworldindata.org/energy-production-consumption (cit. on p. 3).

[2] IAEA, "Climate change and nuclear power 2020," IAEA, Tech. Rep., 2020. [Online]. Available: https://www-pub.iaea.org/MTCD/publications/PDF/PUB1911_web.pdf (cit. on p. 4).

[3] M. para la Transición Ecológica y el Reto Demográfico, "7º plan general de residuos radiactivos," Tech. Rep., 2023 (cit. on p. 4).

[4] P. V. N. G. Station, "Spent fuel pool boron dilution analysis," NRC, Tech. Rep. [Online]. Available: https://www.nrc.gov/docs/ML1731/ML17313A986.pdf (cit. on p. 5).

[5] V. F. de Castro, "A burnup credit methodology for pwr spent fuel storage pool," M.S. thesis, ETSII-UPV, 2012 (cit. on p. 6).

[6] *2030 agenda*. [Online]. Available: https://sdgs.un.org/es/2030agenda (cit. on p. 7).

[7] V. Tarakanov, *What is uranium?* 2023. [Online]. Available: https://www.iaea.org/newscenter/news/what-is-uranium (cit. on p. 9).

[8] *What is spent nuclear fuel?* [Online]. Available: https://www.deepisolation.com/about-nuclear-waste/what-is-spent-nuclear-fuel/ (cit. on pp. 9, 11).

[9] A. D. M. y A. Wilkinson, *Compendium of Chemical Terminology*. IUPAC, 1997 (cit. on p. 12).

[10] D. R. et al., *Química Básica (6ta edición)*. Universidad de Buenos Aires, 2018 (cit. on p. 12).

[11] R. L. Murray, *Nuclear Energy: An Introduction to the Concepts, Systems and Applications of Nuclear Processes*. Butterworth-Heinemann, 2009 (cit. on pp. 12, 13, 15, 18).

[12] *Types and sources of radiation*. [Online]. Available: https://www.cnsc-ccsn.gc.ca/eng/resources/radiation/types-and-sources-of-radiation/ (cit. on pp. 13, 14).

[13] *Ionizing radiation*. [Online]. Available: https://www.osha.gov/ionizing-radiation/health-effects#:~:text=Types%20of%20Health%20Effects,DNA%20(i.e.%2C%20mutations) (cit. on p. 14).

[14] E. Rutherford, "Collisions of particles with light atoms. iv. an anomalous effect in nitrogen," 1919. [Online]. Available: https://web.lemoyne.edu/giunta/RUTHERFORD.HTML (cit. on p. 14).

[15] *What is fission?* [Online]. Available: https://www.open.edu/openlearn/mod/oucontent/view.php?id=26801&section=3.3 (cit. on p. 15).

[16] V. Gopalakrishnan, "Chapter 1 - introduction," in *Physics of Nuclear Reactors*, P. Mohanakrishnan, O. P. Singh, and K. Umasankari, Eds., Academic Press, 2021, pp. 1–86, ISBN: 978-0-12-822441-0. DOI: https://doi.org/10.1016/B978-0-12-822441-0.00001-7. [Online]. Available: https://www.sciencedirect.com/science/article/pii/B9780128224410000017 (cit. on p. 15).

[17] *Nuclear data center at kaeri*. [Online]. Available: https://atom.kaeri.re.kr/nuchart/ (cit. on p. 16).

[18] *Iaea nuclide chart*. [Online]. Available: https://www-nds.iaea.org/relnsd/vcharthtml/VChartHTML.html (cit. on p. 16).

[19] *Japan nuclear data center*. [Online]. Available: https://wwwndc.jaea.go.jp/tools/index.html (cit. on p. 17).

[20] *European nuclear society glossary*. [Online]. Available: https://www.euronuclear.org/glossary/moderator/ (cit. on p. 17).

[21] *Pressurized water reactor (pwr) systems*. [Online]. Available: https://www.nrc.gov/reading-rm/basic-ref/students/for-educators/04.pdf (cit. on pp. 20, 21).

[22] R. Miró and G. Verdú, "Estudio de criticidad de la piscina de combustible gastado región 1. cn trillo i," UPV, Tech. Rep., 2000 (cit. on p. 24).

[23] N. E. Institute, "Guidance for performing criticality analyses of fuel storage at light-water reactor power plants," Nuclear Energy Institute, Tech. Rep., 2019 (cit. on p. 25).

[24] *Criticality requirements for the design of fuel racks* (cit. on p. 25).

[25] *Code of federal regulations (10 cfr)*. [Online]. Available: https://www.nrc.gov/reading-rm/doc-collections/cfr/index.html (cit. on p. 25).

[26] *Scale 6.2.4 user manual*. [Online]. Available: https://scale-manual.ornl.gov/index.html (cit. on pp. 27, 35, 42, 43).

[27] V. Castro, R. Miró, C. Pereira, and G. Verdú, "A burnup credit methodology for pwr spent fuel storage pools: Application to a standard pwr nuclear power plant," *Nuclear Engineering and Design*, vol. 419, p. 112 948, 2024, ISSN: 0029-5493. DOI: https://doi.org/10.1016/j.nucengdes.2024.112948. [Online]. Available: https://www.sciencedirect.com/science/article/pii/S0029549324000505 (cit. on pp. 30, 41).

[28] J. J. Lichtenwalter, S. M. Bowman, M. D. DeHart, and C. M. Hopper, *Criticality Benchmark Guide for LightWater Reactor Fuel in Transportation and Storage Packages*. Oak Ridge National Laboratory, 1997 (cit. on p. 41).

[29] L. I. Kopp and T. Collins, "Guidance on the regulatory requirements for criticality safety analysis of the fuel storage at light-water reactor plants," U. S. Nuclear Regulatory Commission, Tech. Rep., 1998 (cit. on p. 41).

Part III

Budget

To establish the budget and assess the project total costs, the tasks performed and the tools required are considered.

First, the material execution budget will be calculated. This budget is divided into three chapters, each comprising a series of items. Table 5.1 presents these chapters and items, along with their units, measurements, unit prices, and the total cost of material execution. To calculate the hourly costs of workers and the "Software and materials" chapter, its labor and amortization costs are presented in table 5.2 and table 5.3 respectively, assuming a 40-hour workweek and 46 workweeks per year. Labor costs for junior engineer (student) and senior engineer (both tutors) have been obtained from the gross salary tables of a Spanish nuclear engineering company.

Table 5.1: Material execution budget

Chapter	Item	Unit	Measurement	Unit price (€)	Subtotal (€)
1. Work development (junior engineer)	POLARIS modelling	h	35.00	17.44	610.54
	Analysis and validation of the models	h	40.00	17.44	697.76
	MATLAB© scripts creation	h	120.00	17.44	2093.27
	KENO-VI modelling	h	80.00	17.44	1395.51
	Implementation and evaluation of results	h	30.00	17.44	523.32
	Writing the "TFG" document	h	55.00	17.44	959.42
				Junior engineer total (€)	**6279.81**
2. Consultancy (senior engineers)	Specific instruction on nuclear reactor physics	h	80.00	34.19	2734.93
	Consultancy hours	h	150.00	34.19	5127.99
				Senior engineers total (€)	**7862.91**
3. Software and materials	Use of laptop computer	h	360.00	0.2717	97.83
	Use of quasar node	h	185.00	1.3587	251.36
	Use of Microsoft Office 2024	h	70.00	0.0543	3.80
	Use of MATLAB© 2024	h	120.00	0.4891	58.70
	Use of Overleaf license	h	55.00	0.1177	6.47
				Software and materials total (€)	**418.16**
				Material execution budget (€)	**14560.88**

Table 5.2: Amortization hourly costs

Item	Cost (€)	Life span (years)	Hourly cost (€/h)
Laptop computer	2000.00	4	0.2717
Quasar node	7500.00	3	1.3587
Microsoft Office 2024	100.00	1	0.0543
MATLAB© 2024	900.00	1	0.4891
Overleaf license	216.59	1	0.1177

*The SCALE license fees are not included, as access has been granted through the ISIRYM quasar with consent from the developers.

Table 5.3: Labor costs

Worker	**Yearly salary (€)**	**Labor cost (€/h)**
Junior engineer	32096.82	17.44
Senior engineer	62903.30	34.19

To determine the gross budget, 10% for overhead costs and 6% for industrial profit are added to the total material execution cost. A 21% VAT is then applied to the gross budget to obtain the total budget, as illustrated in Table 5.4.

Table 5.4: Total budget

Material execution budget	14560.88
10% Overhead costs	1456.09
6% Industrial profit	873.65
Gross budget	16890.63
21% VAT	3547.03
Total budget (€)	**20437.66**

The total cost of this project amounts to: **TWENTY THOUSAND FOUR HUNDRED AND THIRTY-SEVEN EUROS WITH SIXTY-SIX CENTS**.

Part IV

Annexes

Chapter 6

Annex 1: amu to MeV

The atomic mass unit is defined as one-twelfth the mass of a ^{12}C atom. In order to convert its units to MeV:

Mass of one atom of ^{12}C in grams:

$$12\,\frac{\text{g}}{\text{mol}} \times \frac{1}{6.02214076 \times 10^{23}\text{mol}^{-1}} = 1.99264688 \times 10^{-23}\,\text{g}$$

Mass of one amu in kilograms:

$$1.99264688 \times 10^{-23}\,\text{g} \times \frac{1\,\text{kg}}{1000\,\text{g}} \times \frac{1\,\text{atom of }^{12}\text{C}}{12\,\text{amu}} = 1.660539 \times 10^{-27}\,\frac{\text{kg}}{\text{amu}}$$

Mass-energy equation ($E = mc^2$) to convert kg to J:

$$E = (1.660539 \times 10^{-27}\,\frac{\text{kg}}{\text{amu}}) \times (2.99792458 \times 10^{8}\,\frac{\text{m}}{\text{s}})^2 = 1.492418 \times 10^{-10}\frac{\text{J}}{\text{amu}}$$

As $1\,\text{MeV} \approx 1.60 \times 10^{-13}\,\text{J}$ (Eq. 3.3):

$$1.492418 \times 10^{-10}\frac{\text{J}}{\text{amu}} \times \frac{1\,\text{MeV}}{1.60 \times 10^{-13}\,\text{J}} \approx 931.5\,\frac{\text{MeV}}{\text{amu}}$$

Chapter 7

Annex 2: MATLAB© Script

Script developed for processing and convert isotopes data from POLARIS burnup into KENO-VI composition input in MATLAB©:

```
%% Read .csv file
D = readtable('name_of_file_to_process.csv');
data = table2cell(D);
%% Parameters of the input
axial_level = 1;                                % Nodes [1,32]
dens = 10.5124;
dens_str = sprintf('den=%.4f',dens);
temp = 277;
end_str = "end";
comp_str = sprintf('composition_%d.txt',axial_level); % Composition of "axial_level"
%% Isotopic Filtering
titles = {'case','step','time','power','flux','volume'};
actinides = {'2:u234','2:u235','2:u236','2:u238',...
             '2:np237','2:pu238','2:pu239','2:pu240','2:pu241',...
             '2:pu242','2:am241','2:am243','2:cm242','2:cm243','2:cm244'};
fission_prod = {'1:h001','1:b010','1:b011','1:n014','1:o016','3:kr083','3:nb093',...
                '3:zr094','3:mo095','3:tc099','3:rh103','3:rh105',...
                '3:ru106','3:ag109','3:sn126','3:i135','3:xe131','3:cs133','3:cs134',...
                '3:cs135','3:cs137','3:pr143','3:ce144','3:nd143','3:nd145','3:nd146','3:nd147
                    ','3:pm147',...
                '3:pm148','3:pm149','3:nd148','3:sm147','3:sm149','3:sm150','3:sm151','3:sm152
                    ','3:eu151',...
                '3:eu153','3:eu154','3:eu155','3:gd152','3:gd154','3:gd155','3:gd157','3:gd158
                    ',...
                '3:gd160','3:zr091','3:zr093','3:zr095','3:zr096','3:nb095','3:mo097','3:mo098
                    ','3:mo099',...
                '3:mo100','3:ru101','3:ru102','3:ru103','3:ru104','3:pd105','3:pd107','3:pd108
                    ','3:cd113',...
                '3:in115','3:i127','3:i129','3:xe134','3:la139','3:ba140','3:ce141',...
                '3:ce142','3:ce143','3:pr141','3:nd144','3:sm153','3:eu156'};
% Start of counters i,j
i=1;
j=1;
% Store the data of the titles and the relevant isotopes
while i<size(data,1)
```

```
    a = strfind([titles, actinides, fission_prod],data(i,1));
    if cell2mat(a) == 1
        data_filter(j,:) = data(i,:);
        j=j+1;
    end
    i=i+1;
end
%% Composition creation
header = size(titles,2);
isot_names = data_filter(header+1:end,1);
% Weight of the last t_step (FILTERED)
wt_end_filter = sum(cell2mat(data_filter(header+1:end,end)));
% Isotopic values of the last t_step (grams/total_weight = weight %)
values_out_filter = cell2mat(data_filter(header+1:end,end))./repmat(wt_end_filter,size(
    isot_names));
% Names formatting
names_str_filter = string(isot_names);
delete1 = ["1:","2:","3:"];                     % Delete group identifiers
names_out_filter = replace(names_str_filter,delete1," ");
char_isot = char(names_out_filter);
for i = 1:1:size(char_isot,1)
    for j = 1:1:size(char_isot(i,:),2)
    if isstrprop(char_isot(i,j),'digit') == 1   % Stop in 1st digit
        bf = char_isot(i,1:j-1);                % Get the isotope name
        af = char_isot(i,j:end);                % Get the mass number
        names_out(i,1) = cellstr(string([bf,'-',af]));          % Joints name+'-'+m.number
        break
    end
    end
end
delete2 = ["-00","-0"];                         % Delete null identifiers
names_out = replace(names_out,delete2,"-");
%% Write composition to new file in Keno format
fileID = fopen(comp_str,'w');
for k = 1:1:size(isot_names,1)
    fprintf(fileID,'%s   %d  %s    %e    %d    %s \n',string(names_out(k)),axial_level,
        dens_str,values_out_filter(k),temp,end_str);
end
```